


Hochschule für Angewandte
Wissenschaften Hamburg
*Hamburg University of Applied Sciences*

**Hochschule für Angewandte Wissenschaften Hamburg**

**Fakultät Life Sciences**

# Validation of a Measuring Arrangement for Spectral Response Measurement of Tandem Solar Cells

Master-Thesis

in the study-course

Renewable Energy Systems

submitted by

**Christiane, Dettelbacher**

**2124172**

Hamburg

on 31.03.2014

**Supervisor**: Prof. Dr. Fritz Dildey (HAW Hamburg)

**Supervisor**: Dipl.-Phys. Ulrich Hoyer (ZAE Bayern)

The thesis was supervised and prepared in the laboratory of the institute ZAE Bayern

in colaboration with ZAE Bayen

# Content

# Symbols and constants

| | |
|---|---|
| A | Active area of the cell [m²] |
| AM | Air Mass |
| E | Irradiance [W/m²] |
| EQE | External quantum efficiency |
| FF | Fill factor |
| FWHM | Full width at half maximum |
| HOMO | Highest occupied molecule orbital |
| $I_{SC}$ | Short circuit current |
| ITO | Indium-tin oxide |
| IQE | Internal quantum efficiency |
| $J_{SC}$ | Short circuit current density [A/m²] |
| LED | Light emitting diode |
| LUMO | Lowest unoccupied molecule orbital |
| λ | Wavelength of a photon |
| M | Spectral mismatch factor |
| MPP | Maximum power point |
| P3HT | Poly-(3-hexylthiophene) |
| PCBM | [6,6]-Phenyl-$C_{61}$-butyric acid methyl ester |
| PCE | Power Conversion Efficiency |
| PEDOT:PSS | Poly(3,4-ethylenedioxythiophene) : polystyrene sulfonic acid |
| PV | Photovoltaic |
| $R_S$ | Series resistance |
| $R_{SH}$ | Shunt resistance |
| SMU | Source/Measure Unit |
| SR | Spectral response [A/W] |
| STC | Standard test condition |
| $V_{OC}$ | Open circuit voltage |

# 1 Introduction

Organic solar cells are currently of great interest for research and development. For testing the properties of new developed products in laboratories, the reproduction of the solar spectrum by a solar simulator is required. To enable a more detailed characterisation, different measuring methods have to be applied. A conventional solar simulator can be used to record I-V-characteristics. So far, a separate measuring arrangement is required to measure the spectral response (SR) of solar cells.

As the absorption spectra of organic materials are rather narrow, the tandem technology provides one possibility to enhance the power conversion efficiency (PCE) of organic solar cells. The measurement of the SR is essential, especially for the construction of tandem solar cells. The absorption spectra of both sub cells have to be matched in order to increase the power generation. The SR specifies the magnitude of current generated by photons of each wavelength. The SR curves of a tandem solar cell can provide information about which sub cell is power-limiting and thus help to improve the performance of new devices.

The initial situation of the present study is a solar simulator with LEDs of 22 different wavelengths between 400 and 1050 nm as radiation source. The 22 groups of LEDs with each equal wavelength can be modulated separately by adjusting their intensity between 0 and 100 %. The LED solar simulator and a Source/Measure-Unit (SMU) are both controlled by a software developed in the scope of previous studies at the Zentrum für Angewandte Energieforschung (ZAE) Bayern. The measurement of I-V-curves is validated and a well-established method for the present equipment.

With modulation of the LED irradiation conditions, a method of measuring the spectral response of tandem solar cells should be validated for the present measuring arrangement. This measuring method is novel for solar simulators. The scope of this study includes the calibration of the LED solar simulator by measurement of irradiances for various conditions of illumination as well as testing the suitability of different light intensities of certain wavelengths for the required method.

Organic tandem solar cells are chosen as measuring objects. It should be investigated, how to record and to interpret the SR of organic tandem solar cells under consideration of special characteristics of organic solar cells.

# 2 Organic Photovoltaics

## 2.1 Energy Generation in Organic Solar Cells

The technology of organic solar cells is aspiring due to its great advantages, like for example the low-cost production. The devices can be printed or roll-to-roll-processed. Only a low amount of material is demanded due to very thin layers of about 60 nm. Another advantage of organic solar cells is their usability for new applications. Due to the thin layers, the cells can be built flexible. Various forms, colours, and even semitransparent devices can be produced. This is applicable especially for windows. Also, a variety of materials can be used for organic solar cells and be easily modified in their molecular structure. Thus, a "custom made synthesis" is possible.

In inorganic photovoltaics (PV), the familiar band model specifies the band gaps between two states an electron can have, in the valence band and the conduction band. Under usage of a photon's energy, one electron (negative charge carrier) is lifted from the valence band into the conduction band and leaving a hole (positive charge carrier) in the valence band. By the electrical field, due to donor and acceptor, the charge carriers can be separated and contribute to generation of electrical energy.

In organic photovoltaics, the energy states of the electron are not expressed as valence and conduction band, but highest occupied molecular orbital (HOMO) and lowest unoccupied molecular orbital (LUMO). In a molecule, different orbitals available are occupied by electrons, by degrees from the lowest energy level to the highest energy level. Figure 2.1 shows the energy states in the molecule occupied by electrons. A certain amount of energy is required to lift one electron from HOMO to LUMO, leaving a hole in the HOMO. This determines the energy of the photon, needed to generate a bound electron-hole-pair, called an exciton. The exciton is bound due to Coloumbic attraction.

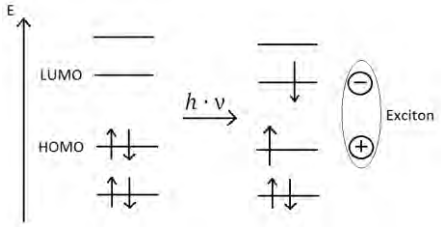


**Figure 2.1:** The process of an electron lifted up to the LUMO and leaving a hole in the HOMO resulting in an exciton

Only the photons with the energy of the band gap can be efficiently utilized in a single-junction solar cell. When the energy of the photon exceeds the energy of the band gap, only a part of its energy corresponding to the energy of the band gap can be converted into free charge carriers. When the energy of the photon falls below the energy of the band gap, this photon cannot contribute to charge separation in the solar cell. The energy E of a photon is determined by its wavelength λ.

$$E = \frac{h \cdot c}{\lambda} \tag{1}$$

## 2.2 Material used for Organic Solar Cells

Organic solar cells are fabricated of organic semiconductors, which consist basically of carbon structures. The organic molecules are formed by a π-conjugated system, which means that the electrons are delocalized in molecule orbitals. The organic solar cell consists, like the inorganic solar cell, of electron-donor and electron-acceptor. Electron-rich conjugated polymers are used as donor and fullerenes as acceptor.

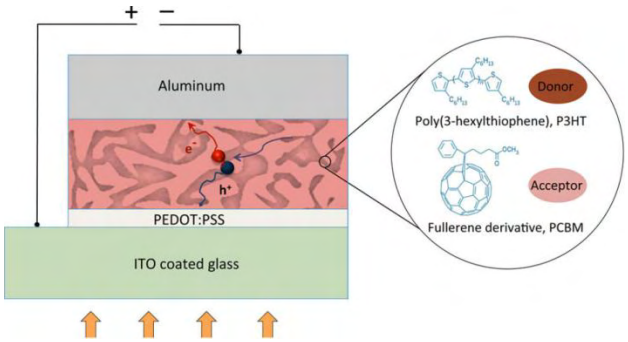


**Figure 2.2:** Bulk hetero-junction of donor and acceptor in an organic solar cell [1]

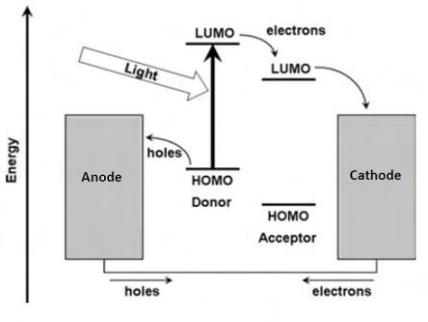


**Figure 2.3:** Appropriate HOMO and LUMO levels of donor and acceptor to enable charge separation [2]

The donor and acceptor combined form the photoactive layer. In the conjugated polymer (donor) the photon is absorbed and the exciton is generated [2]. To separate the exciton into electron and hole, it has to diffuse to the boundary between donor and acceptor. Due to the low diffusion lengths of only about 10 nm, in organic solar cells, the boundary has to be very close to where the exciton is generated. The structure known from inorganic solar cells turns out inappropriate as the electron-hole-pair would recombine before reaching the boundary. Thus for organic solar cells a structure is used, called bulk heterojunction, where the donor and acceptor are mixed. Such a bulk heterojunction solar cell is presented in Figure 2.2. In a heterojunction not only the doping but also materials of donor and acceptor differ from each other.

To enable charge separation "the difference between the HOMO of the donor and the LUMO of the acceptor has to be lower than the potential difference between the bound electron-hole-pair." [3, p. 4] Additionally both HOMO and LUMO level in the acceptor are lower than those in the donor, like shown in Figure 2.3. Thus the electron is forced in the direction of the acceptor and the hole in the direction of the donor pursuing higher energy levels.

For donor material in the most usual case P3HT (Poly-(3-hexylthiophene)) is taken. The acceptor consists of fullerene derivatives, most likely [60]PCBM ( = [6,6]-phenyl-$C_{61}$-butyric acid methyl ester), PCBM in short, due to the high electron affinity of C60. Fullerenes already show sufficient acceptor properties, but PCBM is additionally soluble in chlorobenzene which is important for the production of printable solar cells.

For a built-in electric field a high work function anode and a low work function cathode are used. Their potential difference determines the open circuit voltage ($V_{OC}$) of a solar cell. To ensure ohmic contact and minimize the potential barrier at the active layer/electrode interface, the work functions of the electrodes have to match the LUMO of the acceptor (for the cathode) and the HOMO of the donor (for the anode). [3, p. 6] The front electrode must be transparent in order to minimize the absorption of incoming light. The rear

electrode of the cell consists of Ag, Al or another reflective material to enable absorption of the light in the second pass.

There are two arrangements of the layers possible, the normal and the inverted structure. In the normal structure, the front electrode is the anode. Indium tin oxide (ITO) is used due to its work function (~4.7 eV) which matches the HOMO of P3HT [4]. For the cathode, low work function metals are used, such as Al (4.2 eV), which matches the LUMO of PCBM. To improve the alignment and the ohmic contact between active layer and electrode, interlayers can be inserted. Often a layer of poly(3,4-ethylenedioxythiophene) : polystyrene sulfonic acid (PEDOT:PSS) is inserted between ITO and the active layer.

Furthermore the inverted structure is possible, where the front electrode is the cathode and the rear electrode the anode. To utilize ITO as front and Al as rear electrode interlayers are made use of. N-type metal oxides like TiO2 or ZnO are likely as electron-transporting layer (ETL) between the active layer and the cathode. On the anode sides high work-function transition metal oxides (MoOx, V2O5 or WO3) are used as hole-transporting layer (HTL). With usage of a transition metal oxide interlayer even low work function metals like for example Al can be utilized as anode in inverted organic solar cells. [3, p. 7] Figure 2.4 shows a possible composition of materials used in the normal and the inverted structure.

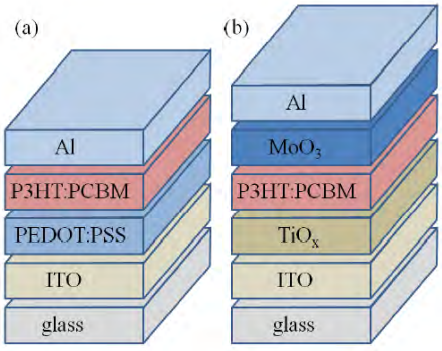


**Figure 2.4:** Normal (a) and inverted (b) structure of organic solar cells [5]

In the normal structure (a) the ITO coated with PEDOT:PSS forms the anode and Al the cathode. In the inverted structure (b) on the other hand, ITO is the cathode and Al the anode. TiOx and MoO3 are electron and hole transporting layers. The active layer in both cases consists of P3HT:PCBM.

There are many reasons for building inverted organic solar cells. One advantage of the inverted structure is its enhanced stability against oxygen and moisture compared to the conventional structure due to avoidance of a low-work function metal top cathode [6] and environmental stability due to avoidance of the highly acidic PEDOT:PSS interfacial layer [7]. Also the construction of semitransparent devices is eased with the inverted structure. This is especially important for multijunction devices. [8 – 10] For the vertical phase separation, the inverted structure is assumed to be more suitable than the regular structure as the P3HT accumulates on top of the film and affects the electron collection at the top electrode. [11] The efficiencies reached with the inverted structure already caught up with the conventional structure. [12 – 15] The EQE of inverted organic solar cells exceeded 70 % whereas the normal structure barely exceeds 60 %. [16]

## 2.3 Organic Tandem Solar Cells

The power conversion efficiency (PCE) of organic single-junction solar cells already exceeded 10 % [17]. Anyway, compared to inorganic solar cells the efficiency of organic solar cells is rather low. The main reason for the limitation is the narrow absorption spectrum of organic solar cells compared to Si or CIS absorbers. [18] As solution for the lack of efficiency, organic tandem solar cells are developed. Figure 2.5 presents the absorption spectra of organic materials. To use a broader range of the solar spectrum in the multijunction-technique two or more cells can be stacked onto each other.

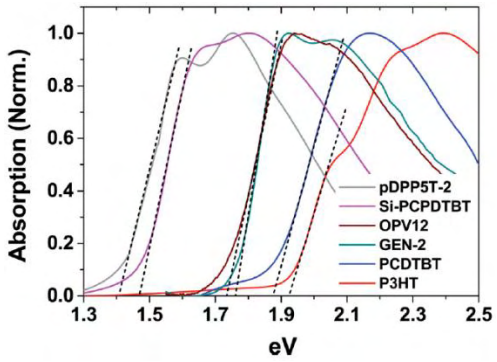


**Figure 2.5:** Absorption spectra of substances used in organic solar cells [19]

A tandem solar cell is a multi-junction solar cell consisting of two sub-cells with complementary absorption spectra. A high band gap front sub cell and a low band gap rear sub cell. As photons with a higher wavelength have larger penetration depths, they are not absorbed in the front sub-cell but can pass until being absorbed in the rear sub cell. The front sub cell thus absorbs the photons with high energy and hence lower penetration depths.

The sub cells can be connected in series or parallel. In the following the concept of the more likely construct, the series connection is considered. The sub-cells are connected in series via an intermediate layer, also called recombination layer. The recombination layer, as already revealed by its term, is a recombination centre for electrons generated in the one sub cell and holes generated in the other sub cell. The chosen material has to minimize ohmic as well as optical losses [20]. The recombination layer also prevents the n-layer on the one sub cell and the p-layer of the other sub cell to build a depletion region when getting in contact. The recombination layer consists of a hole transporting layer and an electron transporting layer. In the most usual case, PEDOT:PSS is taken as hole transporting layer and a n-type metal oxide buffer layer (like ZnO) is taken as electron transporting layer.

Both sub cells should be current-matched, meaning they optimally should both work at their maximum power point (MPP) when the tandem solar cell operate at MPP. In this case, their current densities are equal at their MPP [21]. When the currents of the sub cells are not matched, the charges build up at the recombination layer and limit the $V_{OC}$ [3, p. 10]. Figure 2.6 shows typical I-V-curves of a tandem solar cell and its single-junction solar cells.

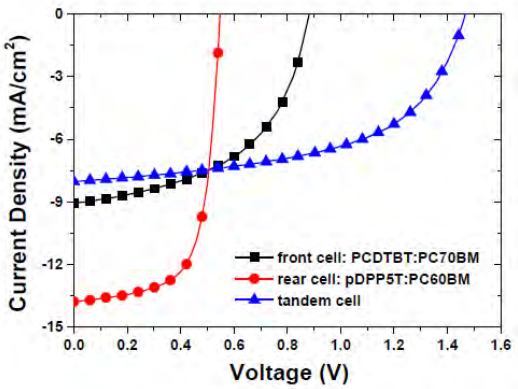


**Figure 2.6:** I-V-curves of a tandem solar cell and its according single-junction solar cells

It can be seen that the current generated by a tandem solar cell is always lower than the lowest current of the single-junction solar cells in the series connection [22]. Otherwise the $V_{OC}$ of the tandem cell is the sum of the open circuit voltages of the sub cells. When designing a tandem solar cell, the rear cell has to be chosen with a higher short circuit current ($I_{SC}$) than the front cell due to the front sub cell limiting the spectrum of light reaching the rear sub cell especially in the low wavelength range. Rough calculations assume theoretical efficiencies of 15% with a bottom sub cell with a band gap of about 1.6 eV and a top sub cell with a band gap of about 1.3 eV. [23] For organic triple-junction solar cells even efficiencies of more than 20% are described [24].

# 3 Spectral Response Measurements

## 3.1 Mathematical Context of Spectral Response and External Quantum Efficiency

Apart from the I-V-curve, one measure to characterize solar cells is the spectral response. The spectral response eases the understanding of recombination processes, collection mechanisms and current generation. The knowledge of the SR is important for example for calculating the spectral mismatch factor. This factor is essential for obtaining the right values for I-V-measurements under standard test condition (STC). The determination of SR is also important for design and development of multi-junction solar cells.

The SR specifies the ratio between generated current and the power incident on the solar cell. [25]

$$SR(\lambda) = \frac{|J_{SC}(\lambda)|}{E(\lambda)} \tag{2}$$

$J_{SC}$ = Short circuit current density [A/m²]

E = Irradiance [W/m²]

The spectral response varies with the wavelength of the irradiation. This is substantiated by the absorption profile of the materials and by the various penetration depths for light of different wavelengths.

In awareness of the SR, also the external quantum efficiency (EQE) and the internal quantum efficiency (IQE) can easily be derived.

$$EQE(\lambda) = \frac{I_{SC}(\lambda)}{q_{el}} \cdot \frac{h \cdot \frac{c}{\lambda}}{E(\lambda) \cdot A_{cell}} = \frac{h \cdot c}{q_{el} \cdot \lambda} \cdot SR(\lambda) \quad (3)$$

C = Vacuum light velocity = 299792458 m/s

$q_{el}$ = Elementary charge of an electron = 1.602176 * $10^{-19}$ C

h = Planck constant = 6.6260695729*$10^{-34}$ Js

The term $\frac{h \cdot c}{q_{el}}$ consisting of three constants can be summarized to 1.24 $\frac{\mu m \cdot W}{A}$. [26] Thus equation 4 can be deduced.

$$EQE(\lambda) = \frac{1.24}{\lambda} \cdot \frac{\mu m \cdot W}{A} \cdot SR(\lambda) \quad (4)$$

The EQE specifies the percentage of photons being converted into useful charge carriers. The IQE however is the ratio between collected charge carriers and the photons that are absorbed by the solar cell, taking into account the reflectivity of the solar cell.

$$IQE(\lambda) = \frac{EQE(\lambda)}{1 - R} \quad (5)$$

R = Rate of reflection

The IQE of organic bulk hetero-junction solar cells can reach 100 % [27].

The spectral response measurement of single-junction solar cells is described in DIN EN 60904-8.

## 3.2 Biasing of the Solar Cell

Biasing, in a broader range of electrical engineering, involves the adjustment of voltages or currents in an electronic circuit to establish proper operating conditions of the electronic components. Involving solar cells, the bias can be generated by two factors, either voltage applied from an outer source or light generating a charge separation inside of the solar cell.

When biasing a solar cell with external voltage, the current is shifted from zero condition. When the cell is not electrically biased, the current is either $I_{SC}$ under illumination, or zero in the dark.

A solar cell can be operated either in forward or reverse bias. When considering the solar cell as a diode, the current generated by illumination is negative. That means it is opposite to the flow direction in a forward

biased diode. The dark I-V-curve shows the behaviour of a diode whose current is growing exponentially with forward bias voltage. Figure 3.1 shows the dark and the illuminated I-V-curve of an organic solar cell. The I-V-curve under illumination is the dark I-V-curve plus the photocurrent (in negative direction) and alterations due to shunt and series resistance. In organic solar cells, the photocurrent is strongly field-dependent. As the diffusion length of the excitons is very small, excitons generated in the neutral region usually recombine. Only the excitons in the depletion region contribute to the generated photocurrent. [29]

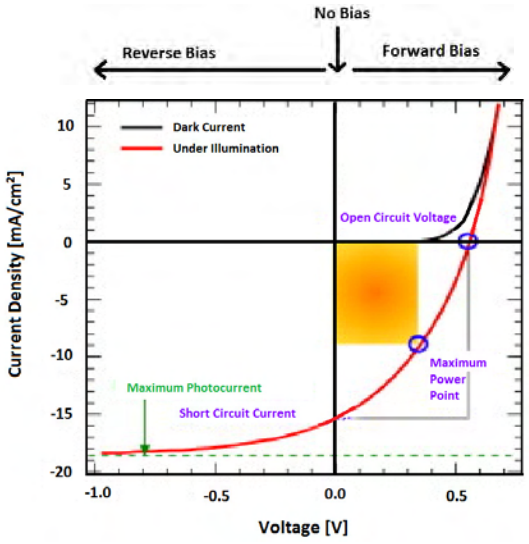


**Figure 3.1:** I-V-curve as a result of voltage biasing of an illuminated solar cell [28]

Forward biasing means that the anode of the solar cell is connected to the positive terminal and the cathode is connected to the negative terminal of a voltage source. The externally applied field is in opposite direction to that in the depletion region. The depletion region is reduced, hence the neutral region enhanced. The driving force to separate the exciton into electron and hole is reduced and thus the photocurrent decreases. When increasing the forward bias up to open circuit voltage ($V_{OC}$) charge separation is not possible any longer. The photocurrent becomes zero.

Reverse biasing means a connection of the anode to the negative terminal and the cathode to the positive terminal of a voltage source. The electrical field of the junction is increased and hence exciton dissociation is enhanced. Unlike in inorganic solar cells, in some organic solar cells the photocurrent can still be increased boyond the value of $I_{SC}$ when biased with reverse voltage. This is especially the case in organic solar cells where exciton dissociation is more difficult. Figure 3.1 shows such behaviour.

The solar cell cannot just be voltage biased but also light biased. Illumination of the solar cell with different irradiances and spectral distributions of light causes different photocurrents. This is important for spectral response measurements. For single-junction solar cells, especially for non-linear ones, biasing with white light is described as mostly necessary to adjust an injection level representing STC. This is essential because carrier lifetimes, photoconductivity, space charge trapping and surface recombination velocities depend on the injection. [30] [31, p. 825]

## 3.3 Spectral Response Measurement of Multi-Junction Cells

The measurement of the SR of tandem solar cells is more complicated than of single-junction solar cells. The design with two terminals is commercially the most attractive one for tandem solar cells. This complicates the measurement of the SR, as there is no access to the intermediate contact. Further aspects, like selecting appropriate bias light and bias voltage ($V_{bias}$), have to be considered. The SR of each sub cell has to be determined separately. Unlike for single-junction solar cells, for the SR measurement of multi-junction solar cells, there is no IEC standard procedure available so far [32].

As the tandem structure is a series connection of both sub cells, only the current flowing through both of the sub cells can be measured. The magnitude of this current is determined by the current limiting sub cell. In order to keep the sub cell to measure current-limiting, the other sub cell is optically biased. The bias light is adjusted to a wavelength, where the absorption of the sub cell to be measured is negligible small in comparison to the absorption of the other sub cell. Thus, the optically biased sub cell creates an excess of charge carriers. While optically biasing the second sub cell with a constant illumination of high intensity, the current-limiting sub cell can be illuminated with monochromatic light of various wavelengths and comparatively low intensity. For each wavelength the short-circuit current is measured. The short circuit current, generated by the first sub cell, can be obtained by subtracting the externally measured short circuit current generated by illumination of just the bias light from the short circuit current generated by the same bias light plus the specific monochromatic light. Thus the error by bias light absorbed in the first sub cell is minimized.

$$I_{SC,mono} = I_{SC,bias+mono} - I_{SC,bias} \tag{6}$$

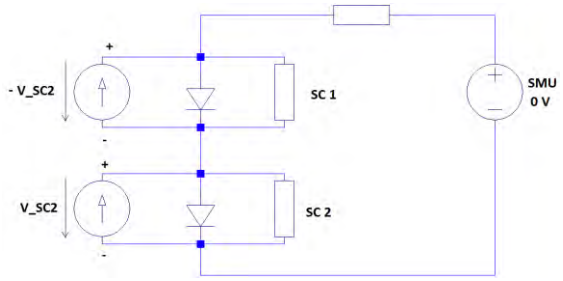


**Figure 3.2:** Equivalent circuit of a tandem solar cell without applying bias voltage

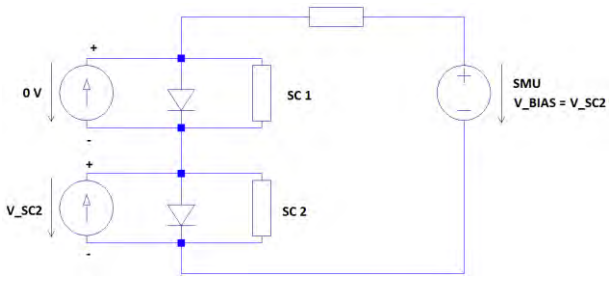


**Figure 3.3:** Equivalent circuit of a tandem solar cell under application of bias voltage

To obtain the spectral response of a sub cell it is essential to measure it in short circuit. Measuring the whole tandem solar cell in short circuit does not include, the sub cell to be measured operating in short circuit as well. The optically biased sub cell operates close to its $V_{OC}$ as it generates excess charge carriers which are prevented from flowing by the current-limiting sub cell. Figure 3.4 shows the current generated by the optically biased sub cell, being way higher than the current generated in the first sub cell under the same illumination. As both sub cells are connected in series and the external voltage is zero, when measuring in short circuit, the first sub cell must operate at the negative value of the voltage the second sub cell operates at. This case can be seen in Figure 3.2. To operate the sub cell to measure in open circuit, an additional

voltage in the magnitude of the $V_{OC}$ of the second sub cell needs to be applied externally, like presented in Figure 3.3. If the open circuit voltages of the sub cells are not known, the $V_{OC}$ of the whole stack can be roughly split according to the wavelength edges of the SR of the sub cells.

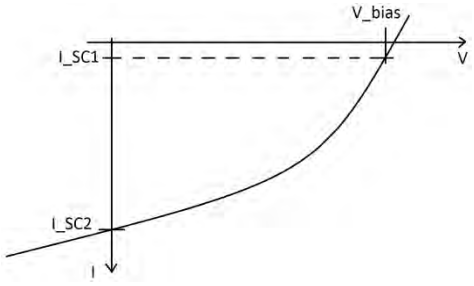


**Figure 3.4:** I-V-curve of the optically biased sub cell, showing the operation close to $V_{OC}$ due to current limitation by the sub cell to measure

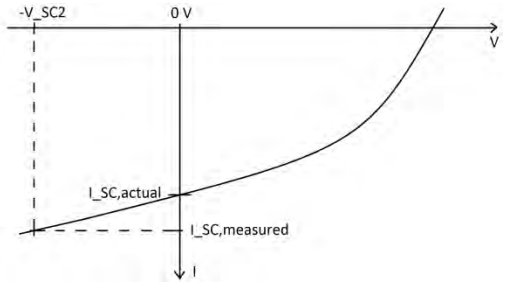


**Figure 3.5:** I-V-curve of the sub cell to be measured, showing the $I_{SC}$ measured without application of bias voltage compared to the actual $I_{SC}$

The error caused by neglecting the bias voltage depends on the slope of the I-V-curve of the tandem solar cell in the range of the $I_{SC}$, especially in reverse bias. Figure 3.5 shows a typical I-V-curve of an organic solar cell. When no bias voltage is applied, the first sub cell is measured at a negative voltage of the magnitude of $V_{bias}$. The current measured is higher than the actual current in short circuit. This leads to overestimation of the SR. [33] In silicon solar cells, however, the slope of the I-V-curve in the range of ISC is very low. Thus, in this case, the bias voltage does not have a big influence.

Unlike in inorganic solar cells, where the effect of the reverse electrical bias is marginal, in organic solar cells measurement errors account up to 16% depending on the material [33].

## 3.4 Set-up for Spectral Response Measurements

A lot of publications refer to already existing set-ups for measuring the SR. For single-junction solar cells the sample is illuminated with continuous white bias light and chopped monochromatic light with comparatively small intensity. Figure 3.6 shows a typical measuring arrangement for single-junction SR measurements.

The monochromatic light is provided mostly by a tustgen filament or a halogen lamp and a downstream monochromator. The light is chopped either before or after the monochromator to generate a certain wavefunction of the monochromatic radiation signal. The chopped monochromatic light generates an AC signal in the sample. By the lock-in-amplifier specifically the magnitude of the AC signal can be determined filtering out the signal by the bias light and noise.

In Figure 3.7 the measuring arrangement for SR of tandem solar cells is presented with bias lights of 780 nm and 532 nm. The solar cell is illuminated with constant bias light whereas the monochromatic light, in this figure emitted by the “lamp”, is chopped to be recorded by the lock-in-amplifier.

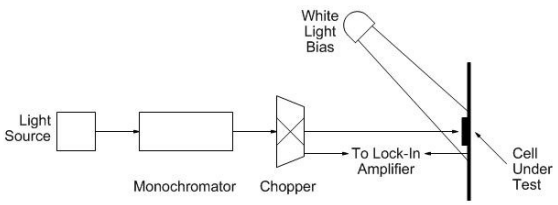


**Figure 3.6:** Simplified structure of a measuring arrangement for SR of single-junction solar cells [34]

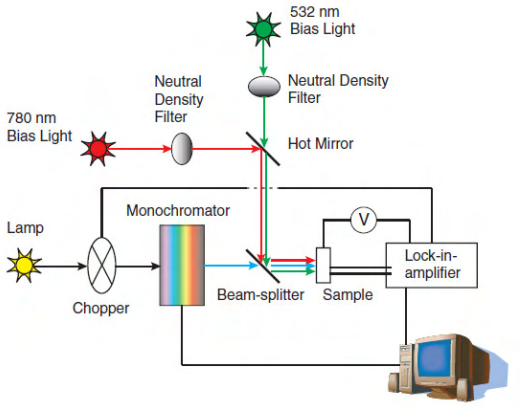


**Figure 3.7:** Measuring arrangement for SR of tandem solar cells [33]

The LED solar simulator provides an alternative to this conventional set-up.

# 4 Materials and Devices

## 4.1 LED Solar Simulator

A solar simulator simulates the spectrum and intensity of the sun for testing solar cells or modules in the laboratory. Depending on the duration of exposure, there exist two different types of solar simulators, flashlight simulators (flasher) and continuous simulators (steady state). Flashlight simulators have a very short duration of exposure of about 10 – 80 ms and are mainly used for testing mono- and multi-crystalline solar cells or modules. The continuous solar simulator provides a steady illumination over a period of time. This is necessary for characterizing materials with longer response times, like for example amorphous silicon thin-film solar cells or organic solar cells. The disadvantage of the long duration of exposure is the heating of the solar cell and therefore measuring inaccuracies.

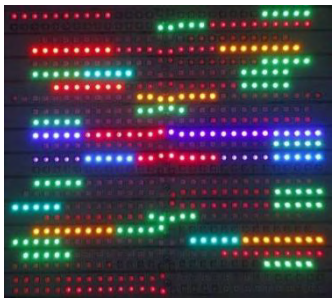

**Figure 4.1:** LED Array used in the solar simulator

In collaboration with ZAE Bayern, the company “FutureLED” developed a LED-based solar simulator. The application of LED-technology provides many advantages, such as low heat impact at a longer duration of exposure and the possibility to be controlled in pulsed operation as well as in steady state. Duration of

exposure between 2 ms and a few minutes is possible. [35] By applying about 700 LEDs with 22 different wavelengths between 400 nm and 1050 nm it is possible to rebuild not only the AM1.5 spectrum, but almost every scenario of illumination. In the following, the LEDs with same wavelengths are defined as one "LED-group". Every LED group can be adjusted separately regarding its intensity. Figure 4.1 shows the LED array contained in the solar simulator.

The LED radiation is conducted through a mirrored light channel for homogenisation purposes and radiated on an area of 18 cm x 20 cm. The LED solar simulator was tested in previous studies to earn class A in all three parameters, spectral match, spatial inhomogeneity and temporal instability regarding to IEC 60904-9. The spectrum emitted by the LED solar simulator is further mentioned in chapter 5.1.

Because of the ability to control the different wavelengths separately, this solar simulator is very suitable for measuring the spectral response of tandem solar cells.

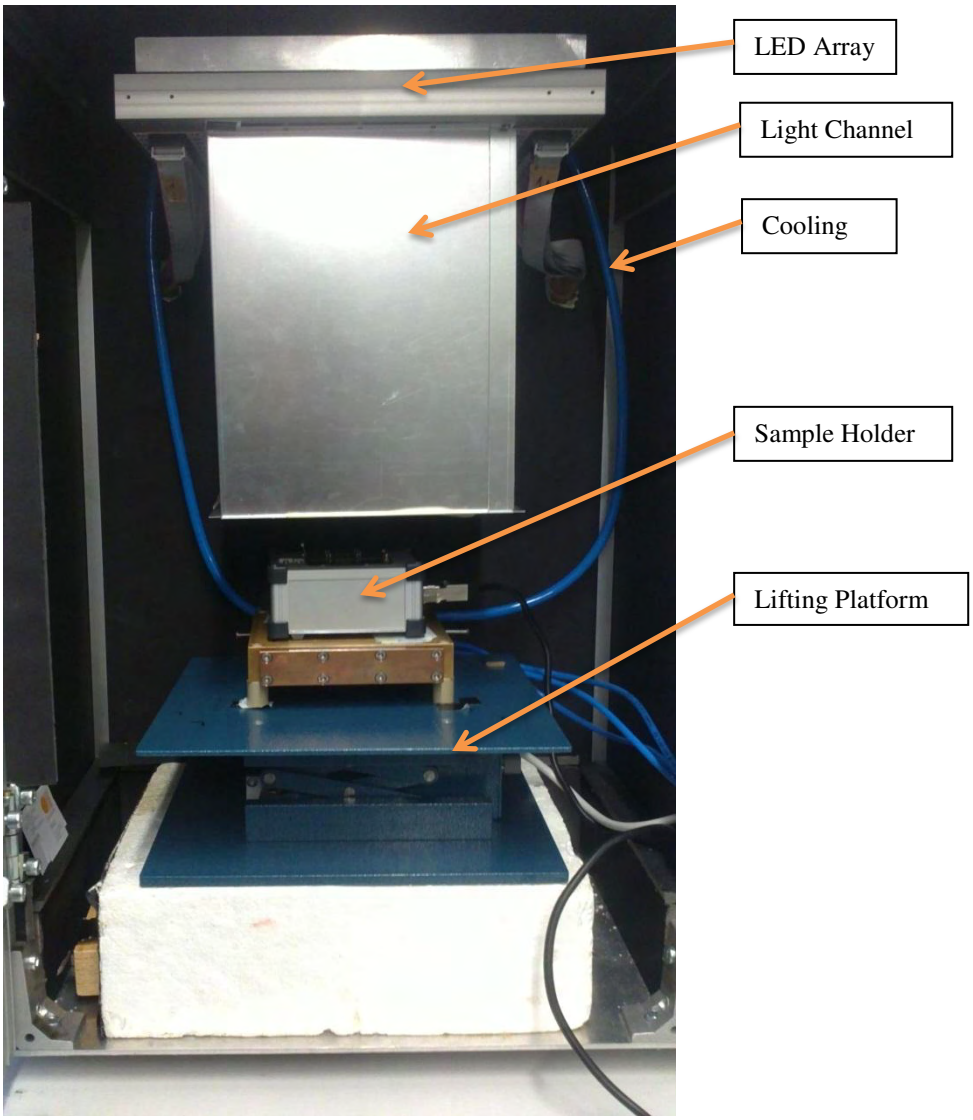


**Figure 4.2:** Measuring arrangement under investigation

The LED array, sample holder and mirrored light channel are enclosed in a blackened box. The sample holder is placed on a lifting platform to adjust the distance between solar cell and light source. To avoid damage of the LEDs, the temperature of the array is controlled by water and an additional pump. The temperature of the sample holder for silicon solar cells is controlled, too. Figure 4.2 shows the structure of the measuring arrangement under investigation. In the following measurements, the sample has a distance to the LED array of 30 cm.

For contacting organic solar cells, a sample holder is used, shown in Figure 4.3. The inverted organic solar cell is contacted by one common cathode but 6 anodes which can be controlled separately. This is further explained in chapter 4.2.

The SMU Agilent B2901A is used to provide external voltage and to measure the current. The measurements are conducted with 2-point-contacting the sample. Usually, for measuring solar cells, 4-point-measurement is used [36]. The error arising by the 2-point measurement is discussed in chapter 8.

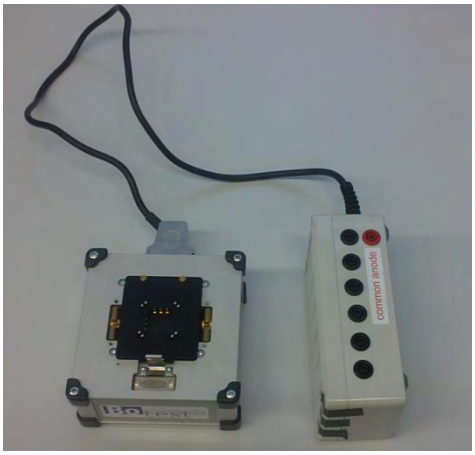


**Figure 4.3:** Sample holder used in the subsequent tests for contacting organic solar cells

In previous studies, the software for controlling the radiation source and the SMU was developed. The upper and lower limit of the voltage and the number of measuring steps can be entered. In order to protect the solar cell and the SMU, a limiting current can be defined. Additional input files for delay and aperture are available. Aperture time is the integration time and delay is the time given for the measuring system to settle. The SMU adjusts a value, then waits the time of the delay [s]. Afterwards, the time of the aperture [s] is taken as measuring time and accordingly the next value is adjusted. In the field of former research projects, different illumination spectra were predefined, inter alia AM 1.5 spectra of different irradiances between 5 and 1000 W/m².

In order to measure the SR, the LEDs provide the bias and also the monochromatic irradiation. The spectrum, emitted by the LEDs, is not monochromatic, but very narrow. Thus in following investigations the spectral bandwidth of the LEDs was considered. The emitted spectra of the LEDs at different wavelengths are measured with a spectrometer. The results are shown in chapter 5.1.

There is a huge advantage of the LED solar simulator in combination with SR measurements. In conventional measuring arrangements, various components like spectral filters, a monochromator and optical chopper are required. In the LED solar simulator the light can easily be adjusted to special demands by varying the intensity of the individual LED groups.

But there are also disadvantages in terms of the LED technology in solar simulators. There is only a limited availability of wavelengths for LEDs. This results in a low number of measuring points and an increased uncertainty due to interpolation between the measuring points in the SR measurements. There is another disadvantage with special regard to the LED solar simulator under investigation. The irradiance of the LEDs is just enough to reach 1000 W/m² under full capacity utilization of various wavelengths. This particularly affects the utilization for SR measurements, due to different light sources having to be provided by the LEDs. Thus there is only small margin for adjusting light parameters. This is exposed in detail in chapter 6.

## 4.2 Solar Cells under Investigation

**Organic Solar Cells (I-Meet)**

One organic tandem solar cell and two single-junction solar cells representing the two sub cells of the tandem solar cell are used as main devices under investigation. The samples were provided by co-workers of the ZAE and I-Meet, a department of the Friedrich Alexander University in Erlangen. The single-junction solar cells are used to obtain the wavelength of the bias light for the tandem solar cell and to get results of the SR comparable to the measured data of the tandem solar cell.

The layers used in the single-junction solar cells are ITO/ZnO/pDPP5T-2:PCBM/MoOx/Ag and ITO/ZnO/PCDTBT:PCBM/MoOx/Ag. The thickness of the active layer is always optimized in regard to the structure. In the single-junction solar cells the PCDTBT layer is 80 nm and the pDPP5T-2 layer is 100 - 120 nm.

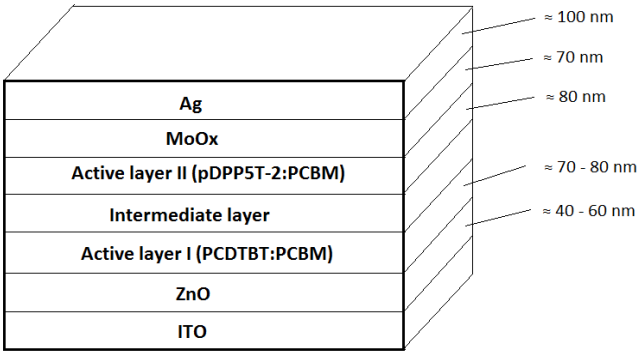


**Figure 4.4:** Layers of the organic tandem solar cell used as measuring object

The structure of the tandem solar cells is similar, but with an additional intermediate layer and both active layers. However, the optimization of the active layer thickness is more complex in the tandem structure.

When varying the active layer thickness of both sub cells, the number of photons absorbed in each sub cell changes. Isolines arise where the photons absorbed in the top sub cell and the bottom sub cell are equal. This condition has to be fulfilled in order to keep the tandem solar cell current-matched. Figure 4.4 displays the different layers of the tandem solar and their respective thickness.

On one cell substrate, there are six so called cells, each with an own anode, consisting of Ag, and a common cathode, made of ITO. The different layers are applied to ITO-covered glass. Anode and cathode are electrically separated by laser patterning. Each of the cells has an active area of 10.4 mm² [19]. Only the charge carriers, generated in the active layer in close proximity to the electrode, can contribute to the generated current. As low band-gap polymer, pDPP5T-2 blended with PC60BM is taken, while the high band-gap polymer is PCDTBT blended with PC60BM. The intermediate layer consists of PEDOT:PSS/ZnO.

Figure 4.5 shows the three organic solar cell samples under investigation. The colour of the active layer indicates the type of solar cell. The single-junction solar cells consist of only one active layer, which is in the present cases green (pDPP5T-2) and red (PCDTBT). The tandem solar cell owns both layers of the single-junction solar cells.

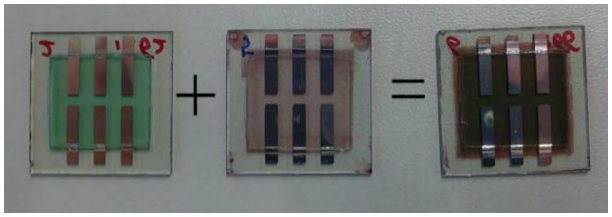

**Figure 4.5:** Organic solar cells used in the following tests

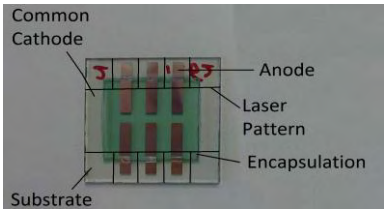


**Figure 4.6:** Contacting elements and encapsulation of the organic solar cell

To avoid degradation due to reaction between the active layer and oxygen, the components are encapsulated in an impermeable package. In Figure 4.6, the components of organic solar cells are demonstrated.

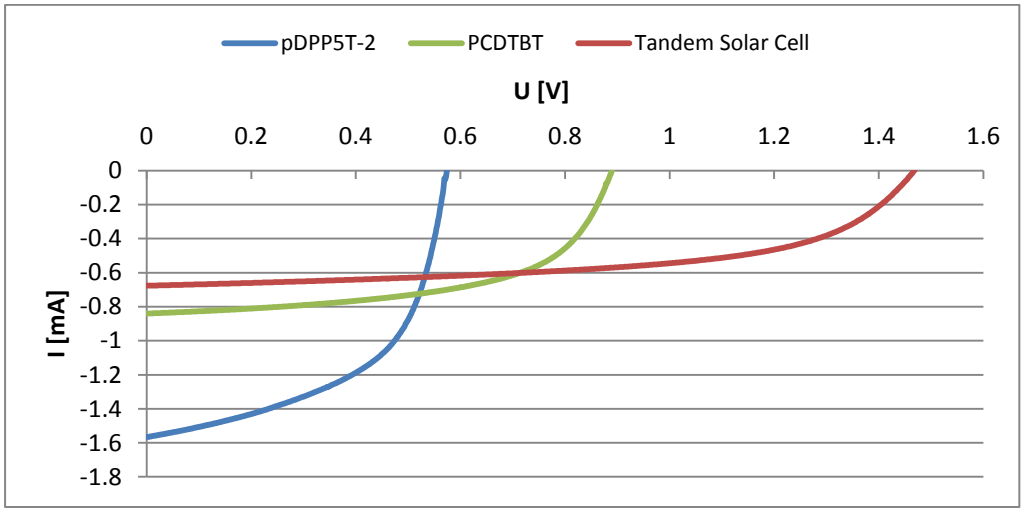


**Figure 4.7:** Characteristic curves of the three organic solar cells under investigation

The organic solar cells are stored in the dark at room temperature. An excessive exposure to light encourages degradation of the organic devices. For minimizing the effect of degradation on the results of the SR-measurements, regular measurements were taken for all three cell substrates, to observe the stability of their performance. In the following, just one cell of each substrate, which showed the most stable behaviour over the whole period, is investigated. Figure 4.7 represents the I-V-curves of the tandem solar cell and the respective single-junction solar cells. The current of the tandem solar cell is lower than the currents of the sub cells, but the voltage sums up. The tandem solar cell technology enhances the power yield. The tandem solar cell generates 0.57 mW, while the PCDTBT single-junction solar cell generates only 0.43 mW and the pDPP5T-2 only 0.49 mW under STC. Hence, also the PCE of the solar cells can be calculated. As the I-V-curve is measured under STC, the irradiance is 1000 W/m². Equation 7 describes the calculation of the PCE for the present case.

$$\mathrm{PCE} = \frac{\mathrm{P_{irr}}}{\mathrm{P_{sc}}} = \frac{\mathrm{E_{irr}} \cdot \mathrm{A} = 1000\ \frac{\mathrm{W}}{\mathrm{m^2}} \cdot 10.4 \cdot 10^{-6}\ \mathrm{m^2}}{\mathrm{P_{SC}}} \tag{7}$$

A = Active area of the cell [m²]

The PCE is 5.44 % for the tandem solar cell, 4.14 % for the PCDTBT single-junction solar cell and 4.67 % for the pDPP5T-2 single-junction solar cell. This demonstrates how the efficiency can be increased due to the tandem technology.

Especially the characteristic curve of the pDPP5T-2 sub cell shows a strong slope close to the $I_{SC}$. This signifies a low shunt resistance ($R_{SH}$). The tandem solar cell especially has a comparatively high series resistance ($R_S$), which expresses in a strong slope of the I-V-curve close to the $V_{OC}$.

**Organic Solar Cells (KIT)**

Further samples are provided by the Karsruher Institut für Technologie (KIT). Organic solar cells can be fabricated in countless designs. The samples fabricated at the KIT contain four cells, each with an own anode and cathode. KIT delivered two single-junction solar cells with active layers consisting of P3HT:IC[60]BA and PSBTBT:PC[71]BM and two tandem solar cells with both active layers. Comparable EQE data and I-V-characteristics are made available by KIT.

**Reference Cell**

For calibration purposes, a mono-crystalline silicon solar cell is used as reference cell. As solar cells with different absorption spectra are measured, a reference cell, whose SR covers the whole range of the wavelengths, emitted by the LED solar simulator, is used. This kind of solar cell is very applicable for calibration procedures as its SR function is quite steady without abrupt changes.

**Silicon Tandem Solar Cell**

To explain effects, occurring during SR measurements, a tandem solar cell is simulated by two silicon solar cells connected in series, each furnished with another spectral filter. The filter with blue colour, on the right side in Figure 4.8, has its central wavelength at 507 nm with a full width at half maximum (FWHM) of 210 nm (Edmund Optics, BG-39 1" D.) and the other filter with black colour, on the left side in Figure 4.8, has its central wavelength at 830 nm with a FWHM of 260 nm (Edmund Optics, RT-830 1" D.). Therefore, small blades (d = 23 mm) are laser-cut out of a silicon solar cell. The connectors are soldered on the bus-bars. To reduce the shunts due to the laser process, the edges of the silicon blades are filed off.

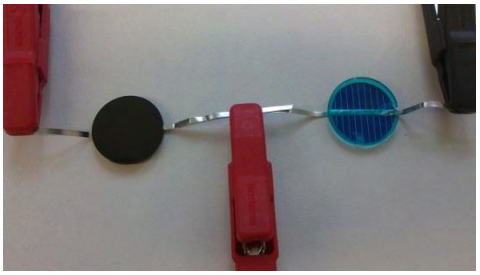

**Figure 4.8:** Hand-made silicon tandem solar cell

# 5 Calibration of the LED Solar Simulator

## 5.1 Calibration with Spectrometer

To obtain the spectral shape of the radiation emitted by the LEDs and the accuracy of the rebuild AM 1.5 test spectrum, the spectrometer Black-CXR-SR-50 from "StellarNet" (UV-VIS-NIR range) is used. Due to improper calibration of the spectrometer, a correction factor is applied, such that the measured spectrum equals the integral of AM 1.5 at 1000 W/m² for wavelengths between 378.5 and 950 nm. The measurement of the $I_{SC}$ of the reference cell with the test spectrum lies within the tolerance. Thus, similar irradiances of the test spectrum and the reference spectrum are accepted. In Figure 5.1 the AM 1.5 (1000 W/m²) norm spectrum and the spectrum generated by the LED solar simulator are opposed.

With this data, the spectral match between the AM1.5 STC spectrum (according to IEC 60904-3 (1989) part III) and the spectrum of the LED solar simulator can be calculated according to IEC 60904-9. Even for solar simulator classified as class A, corrections for the spectral match are necessary.

In Figure 5.1 can be seen, that the measurements at wavelengths >900 nm are inaccurate and strongly influenced by noise. At wavelengths >1050 nm, no signal can be detected. Therefore, for calculating the spectral match, this range is not considered and assumed to perfectly fit the norm spectrum. Table 1 represents the spectral match of the test spectrum of the LED solar simulator.

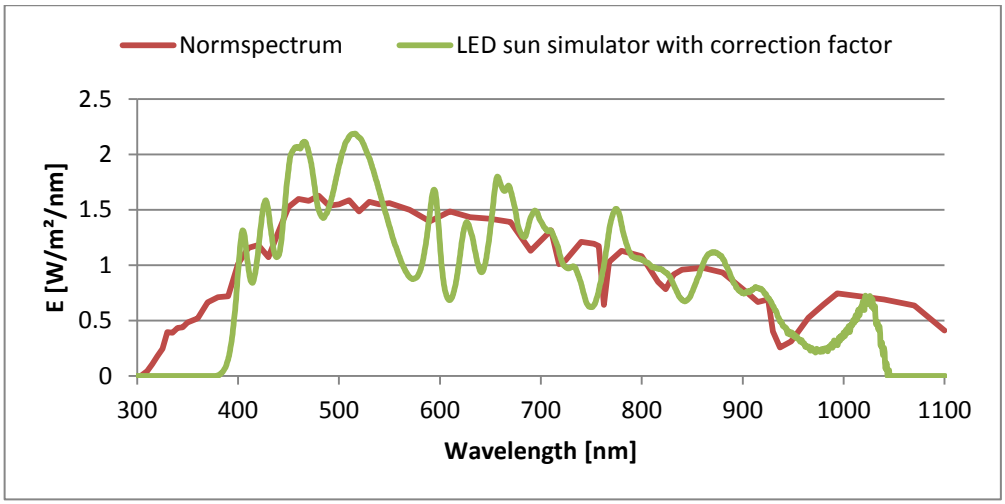


**Figure 5.1:** Spectrum of the LED solar simulator at AM 1.5, 1000 W/m² compared to norm spectrum

For values of spectral match between 0.75 and 1.25, the solar simulator is defined as class A. Neglecting the range from 900 – 1100 nm, the LED solar simulator can be classified as "class A" according to IEC 60904-9.

The spectral mismatch factor is always regarded to one specific solar cell and can be calculated according to IEC 60904-7. Therefore the SR of this solar cell needs to be known. The calculations for the spectral mismatch are described in chapter 6.2 and 7.4. The spectral mismatch gives the effect of the deviation between the test spectrum (green line in Figure 5.1) and the reference spectrum (red line in Figure 5.1) for the solar cell under test.

**Table 1:** Spectral match related to interval regarding to IEC 60904-9

| Wavelength in range nm | Percentage of total irradiance in the wavelength range 400 nm – 1100 nm (STC) | Recorded percentages at LED solar simulator | Spectral match to all intervals |
|---|---|---|---|
| 400 – 500 | 18.4 % | 20.14 % | 1.0946 |
| 500 – 600 | 19.9 % | 20.49 % | 1.0300 |
| 600 – 700 | 18.4 % | 16.93 % | 0.9200 |
| 700 – 800 | 14.9 % | 14.30 % | 0.9601 |
| 800 – 900 | 12.5 % | 12.23 % | 0.9783 |
| 900 – 1100 | 15.9 % | 15.9 % (assumed) | 1 (assumed) |

Additionally, the spectrum of the irradiation of the individual LED groups is recorded. Figure 5.2 shows the light spectra, emitted by each LED group at 100 % intensity. The spectrum of the LEDs with 1050 nm cannot be recorded and the spectrum of 1020 nm is strongly influenced by noise due to limitations in silicon sensors.

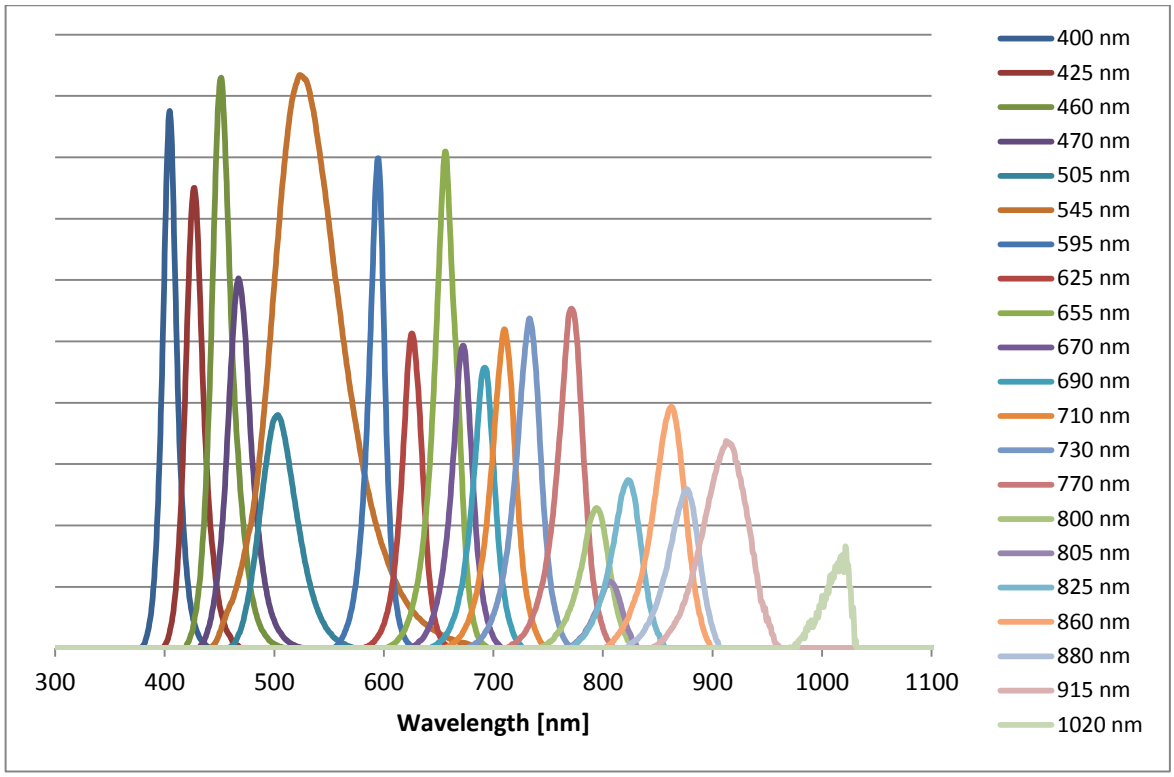


**Figure 5.2:** Radiation spectra of each LED group at their maximum power

The FWHM of the LEDs at 100 % of their power can amount up to 71 nm (for the LED group of 545 nm). Average FWHMs are about 25 nm. A full table of the FWHM of all LED groups at 100 % of their intensity can be found in appendix A. For lower intensities, the bandwidth is decreasing. The spectral shape of the emitted light is considered when calibrating the LED solar simulator. In the following, anyway, the light emitted by just one LED group will be mentioned as “monochromatic”.

Due to the limitation in high wavelength range and the insufficient calibration of the spectrometer, for calibration of the LED solar simulator, additionally a reference cell has to be used.

## 5.2 Calibration with Reference Cell

**Irradiance of the LED groups**

A reference cell with given SR for wavelengths between 300 and 1185 nm is used to determine the irradiance of the LED groups at a certain percentages of their intensity. The calibration certificate of the reference cell can be found in appendix B. The measurements of the calibration lab were conducted with a white bias illumination generating a bias current of 10 mA. To reproduce this condition, an appropriate pre-programmed AM 1.5 spectrum is selected. A bias current of 10.3 mA is yielded with 73 W/m². Additionally, certain intensities of the specific wavelengths are added to the white bias light. For each condition of illumination, the $I_{SC}$ generated additional to the bias current is measured. The irradiance of one specific wavelength and intensity can be calculated by equation 8.

$$E(\lambda, \%) = \frac{|I_{SC}(\lambda, \%)|}{SR(\lambda)} \tag{8}$$

The spectral distribution of the radiation emitted by each LED group is determined in chapter 5.1. When illuminating the solar cell with "monochromatic" light, the current induced is not generated by only one central wavelength, but from all wavelengths in the emission spectrum by a certain amount. Thus, to obtain the real irradiance, all SR of the reference cell inside this spectral range are considered. Figure 5.3 shows the emission spectra of one LED group at 505 nm and the variation of the SR of the reference cell in this range. The spectral distribution is normalized to 1 at its peak.

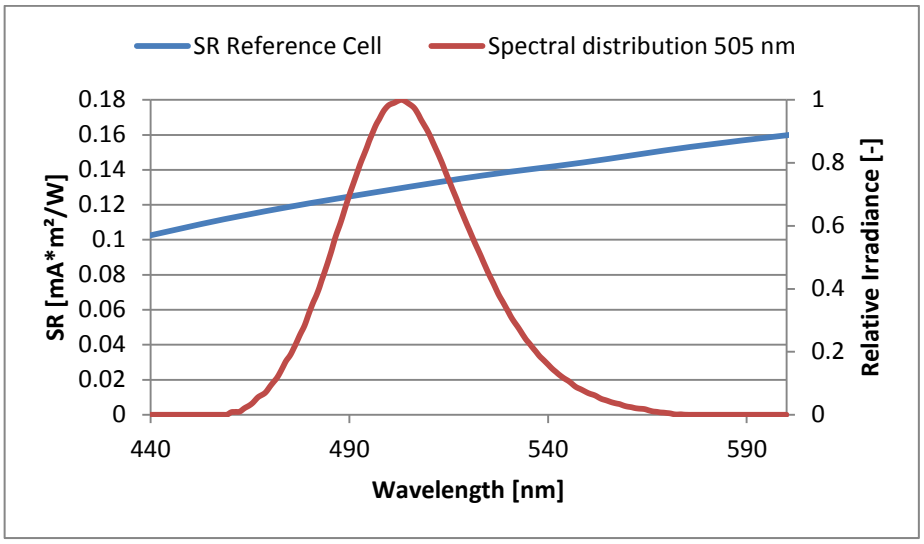


**Figure 5.3:** Regression of the SR in the range of the spectral bandwidth of a LED

Thus, equation 8 is not sufficient for calculating the irradiance of one LED group at a specific intensity. Instead, the short circuit current measured depends on the relative irradiances and the SR at the regarding wavelengths.

$$I_{SC,Ref} = \alpha \cdot \int_{\lambda_{min}}^{\lambda_{max}} E_{RI}(\lambda) \cdot SR_{Ref}(\lambda) d\lambda \tag{9}$$

$E_{RI}$ = Relative irradiance

The constant factor α is required, as the absolute irradiance at the specific wavelengths is not known, but just the spectral distribution. For each wavelength and intensity an individual α is calculated by equation 9.

To obtain the whole irradiance of one LED group, reduced to one monochromatic point, equation 10 is used. It summarizes the relative irradiances at the occurring wavelengths and the constant factor α.

$$E(\lambda_{mono}) = \alpha \cdot \int_{\lambda_{min}}^{\lambda_{max}} E_{RI}(\lambda)\, d\lambda \tag{10}$$

The integrals are solved by the numerical method "The rectangle-procedure" (equation 11).

$$\int_{\lambda_1}^{\lambda_2} f(\lambda)d\lambda = \sum_{i=\lambda_1}^{\lambda_2} 0.5 \cdot (\lambda_{i+1} - \lambda_i) \cdot \left(f(\lambda_i) + f(\lambda_{i+1})\right) \tag{11}$$

For the LEDs of 1020 and 1050 nm, the shape of the emission spectrum could not be considered for determining the irradiance. Instead, they were assumed to be monochromatic under use of equation 8.

**Linearity of the irradiance at different LED groups**

As a certain capacity of the LEDs' irradiance is required to provide the white bias light, the irradiance of the LEDs could not be calibrated at 100 % of their intensity. The irradiances exceeding 80 % intensity can only be approximated by extrapolating the curves of irradiance depending on percentage of power. This method, anyway, gives only rough assumptions and cannot be verified. Two typical cases of regression are represented in Figure 5.4 and Figure 5.5. The 505 nm LED group shows a sub-linear behaviour, whereas the 770 nm LED group demonstrates linear behaviour of the irradiance.

The non-linear behaviour can be explained by the changes in spectral distribution of the emission spectra at different intensities.

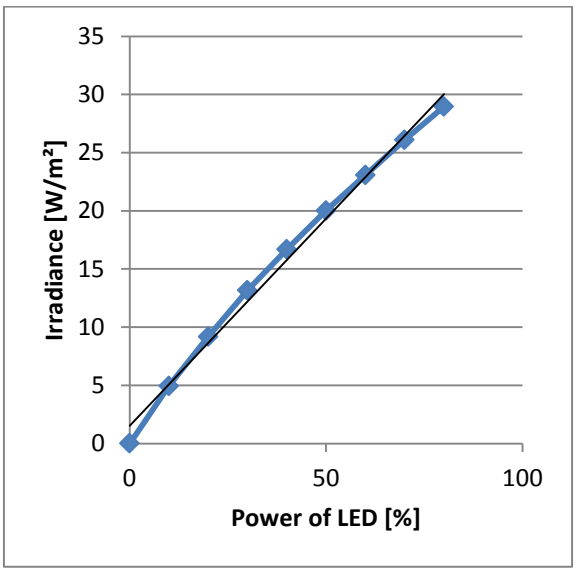


**Figure 5.4:** Irradiance of the 505 nm LED group depending on the percentage of their maximum power revealing sub-linear behaviour

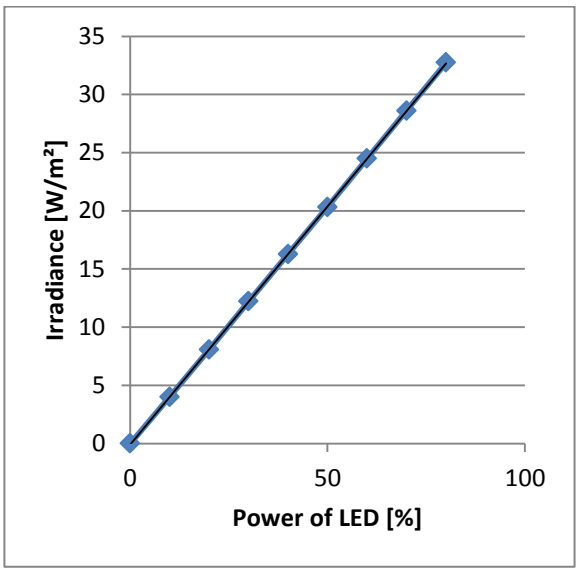


**Figure 5.5:** Irradiance of the 770 nm LED group depending on the percentage of their maximum power revealing linear behaviour

When measuring the SR, both illumination sources, the bias light and the monochromatic light are provided by the LED array. However, for calculating the SR according to equation 2, only the irradiance of the monochromatic light and the proportion of the $I_{SC}$ generated by the monochromatic light are required. Thus,

for applying bias light and monochromatic light of the same wavelength, the regression behaviour of the irradiance must be considered. For example, when providing bias light with 60 % of a certain wavelength and adding 20 % intensity of monochromatic light, the irradiance at 80 % minus the irradiance at 60 % states the right irradiance of the monochromatic light.

For the following measurements, the irradiance of the monochromatic light can be obtained by equation 12.

$$E_{mono} = E(I_{bias+mono}) - E(I_{bias}) \tag{12}$$

**Magnitude of pre-programmed test spectrum AM 1.5**

The reference cell is also used to examine the irradiance of the pre-programmed test spectrum (AM 1.5, 1000 W/m²). In doing so, the $I_{SC}$ of the reference cell is measured and compared to the $I_{SC}$ given from the calibration lab. The obtained value appears in the tolerance range.

# 6 Characterisation of Single-Junction Solar Cells

## 6.1 Spectral Response of Single-Junction Solar Cells

**Linearity of the Measuring Objects**

Organic solar cells have a reputation for not being linear [33]. Linearity means, that the SR at a certain wavelength is constant and does not depend on the intensity of the illumination. Hence, the $I_{SC}$ generated in the sample would have to behave proportional to the irradiance. The linearity is calculated according to DIN EN 60904-10. The sample is illuminated with white bias light of different irradiances from 0 to 1000 W/m², provided by the pre-programmed AM 1.5 test spectra. For deviations between the measuring points and the regression line smaller than 2%, the measuring object can be considered as linear. For the present measuring objects, the condition of linearity is not fulfilled

The strong deviations from linearity at small irradiances, which occur for both single-junction solar cells, can be traced back to noise. The magnitude of the noise is described in chapter 8. Also, the irradiances of the pre-programmed AM1.5 spectra were calibrated with a silicon reference cell. This leads to a spectral mismatch for organic solar cells. Hence, the linearity, tested with the LED solar simulator, is considered as inaccurate.

**Measuring with White Bias Light**

According to DIN EN 60904-8, the SR of non-linear solar cells has to be tested with white bias illumination of spectral distribution similar to AM1.5. In the following tests, the monochromatic and the white bias light are both provided by the LED array of the solar simulator.

Two measuring steps are necessary to obtain the SR. In the first step, the sample is illuminated with monochromatic light plus bias light, in the second step just bias light is applied. The current generated in the second step is subtracted from the current measured in the first step. Both light sources are continuous. There is no chopper in the present measuring equipment.

To obtain the SR at one of the 22 wavelengths, the $I_{SC}$ generated by the white bias light is subtracted from the $I_{SC}$ measured with monochromatic light plus white bias light. The remaining current is divided by the irradiance of the monochromatic light to obtain the SR in $\frac{A \cdot m^2}{W}$. Division by the active area of the solar cell leads to the SR in $\frac{A}{W}$.

$$SR(\lambda) = \frac{\left|I_{SC,mono+bias}(\lambda) - I_{SC,bias}(\lambda)\right|}{E_{mono}(\lambda) \cdot A} = \frac{|\Delta I_{SC}(\lambda)|}{E_{mono}(\lambda) \cdot A} \tag{13}$$

The SR can be plotted in a diagram, depending on the wavelength of the monochromatic light.

The white bias illumination should range from 0 – 1000 W/m². [37] In the following measurements the pre-programmed AM1.5 spectra between 0 and 675 (respectively 800 W/m²) are used as white bias light. Further enhancement of the irradiance is not possible, as a certain capacity of the LED intensity is required to provide the monochromatic light. 20 % (respectively 5 %) of intensity is added to each wavelength successively, serving as monochromatic light. The measured values are inserted in formula 13.

Figure 6.1 - Figure 6.4 show the SR depending on the irradiance of white bias light. In Figure 6.1 and Figure 6.2, the SR of the pDPP5T-2 single-junction solar cell is investigated with 20 % and 5 % intensity of monochromatic illumination. Figure 6.3 and Figure 6.4 represent the characteristics for the PCDTBT single-junction solar cell under the same conditions. The irradiance of the white bias light is given in the legend.

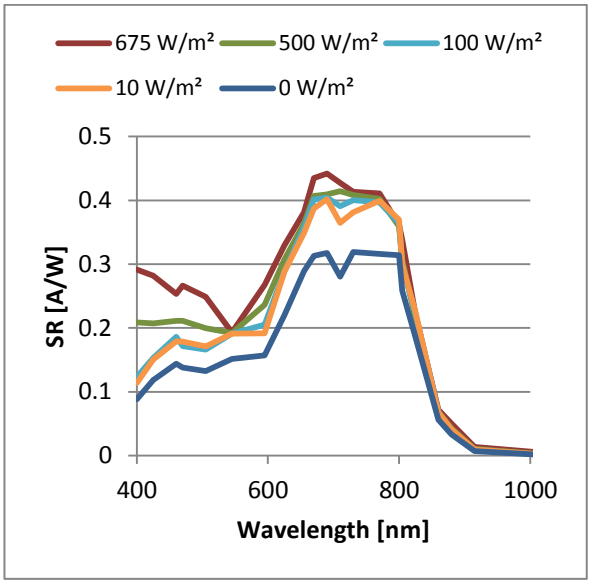


**Figure 6.1:** SR of the pDPP5T-2 single-junction solar cell under monochromatic illumination of 20 % intensity depending of the irradiance of the bias light

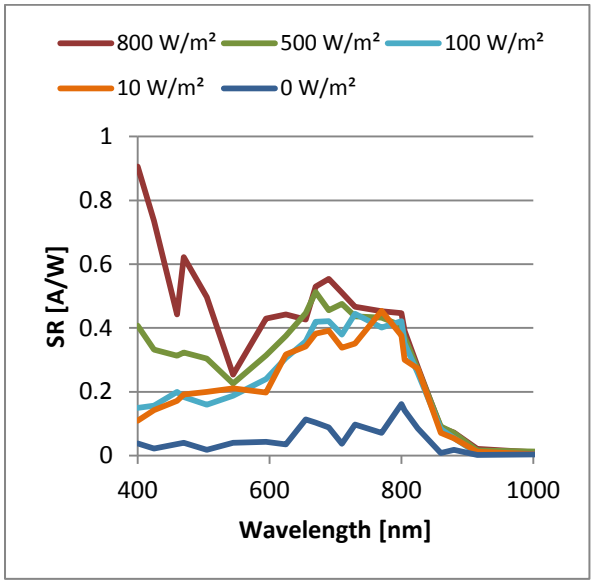


**Figure 6.2:** SR of the pDPP5T-2 single-junction solar cell under monochromatic illumination of 5 % intensity depending of the irradiance of the bias light

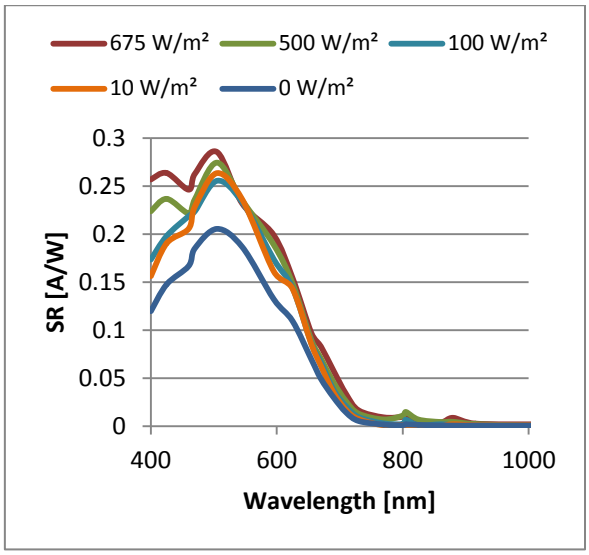


**Figure 6.3:** SR of the PCDTBT single-junction solar cell under monochromatic illumination of 20 % intensity depending of the irradiance of the bias light

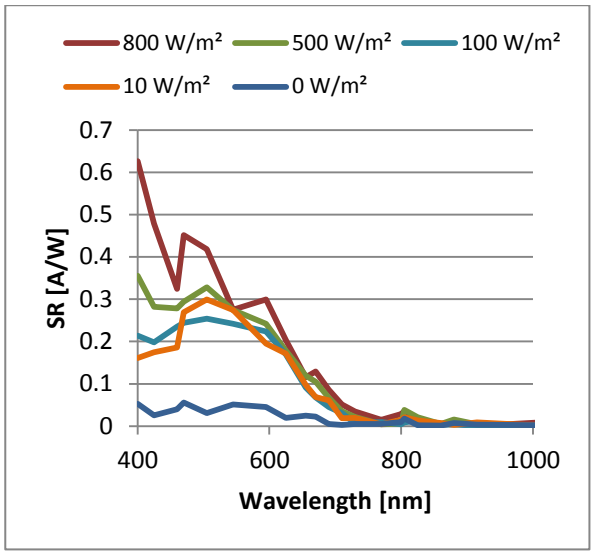


**Figure 6.4:** SR of the PCDTBT single-junction solar cell under monochromatic illumination of 5 % intensity depending of the irradiance of the bias light

For both single-junction solar cells, a slight increase in SR with increasing white bias light can be observed. Only monochromatic light with 20 % intensity is not enough to saturate the solar cell. Anyway, the curves are not clearly defined and disturbed by noise. It is remarkable, that the SR in the low wavelength range increases for higher white bias light irradiances.

Also, a silicon solar cell and another organic single-junction solar cell (P3HT:PCBM) are measured with different intensities of white bias light. For all solar cells, a increase in the range of short wavelengths can be recognized for higher white bias light irradiations. The similatity in bahaviour of all measured solar cells indicates a systematic measurement error.

The distortions of the characteristics are assumed to be caused by the lack of intesity of monochromatic light. For 5 % (Figure 6.2 and Figure 6.4) monochromatic light the detected signals are lower than for 20 % (Figure 6.1 and Figure 6.3) monochromatic light intensity. They also are more influenced by noise. With application of white bias light, no proper SR curve can be made out.

**Measuring without White Bias Light**

Measuring with white bias light is not reliable for the present measuring arrangement. Thus, this method should be omitted. In the following tests, the organic single-junction solar cells are illuminated with just monochromatic light to measure the SR. Equation 13 can be simplified to equation 14.

$$SR(\lambda) = \frac{\left|I_{SC,mono}(\lambda)\right|}{E(\lambda) \cdot A} \tag{14}$$

Figure 6.5 and Figure 6.6 show the SR of the two single-junction solar cells irradiated with monochromatic light of different intensities.

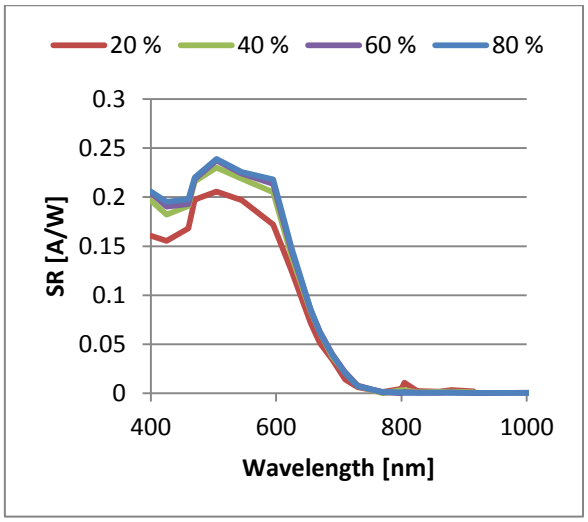


**Figure 6.5:** PCDTBT single-junction solar cell under monochromatic irradiation of different intensities

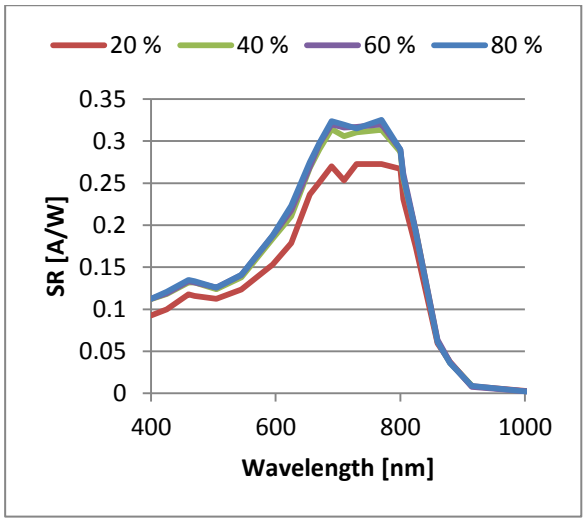


**Figure 6.6:** pDPP5T-2 single-junction solar cell under monochromatic irradiation of different intensities

For higher intensities of monochromatic light, the SR approximates a saturation level. With an intensity of 80 %, the curve is not significantly increased compared to the data of 60 % monochromatic light intensity. Hence, the solar cell is assumed as saturated, and the SR data as reliable.

The appropriate bias light wavelengths for the tandem solar cell measurement can be obtained from all measurements. At those wavelengths, the absorption of one sub cell is maximal, whereas the other sub cell absorbs marginally. When applying the SR of both single-junction solar cells in one diagram, like it can be seen in Figure 6.7, the appropriate bias light wavelengths can easily be obtained. For measuring the pDPP5T-2 sub cell, the tandem solar cell should be irradiated with bias light of 505 nm. When measuring the PCDTBT sub cell, a bias light of 770 nm must be selected.

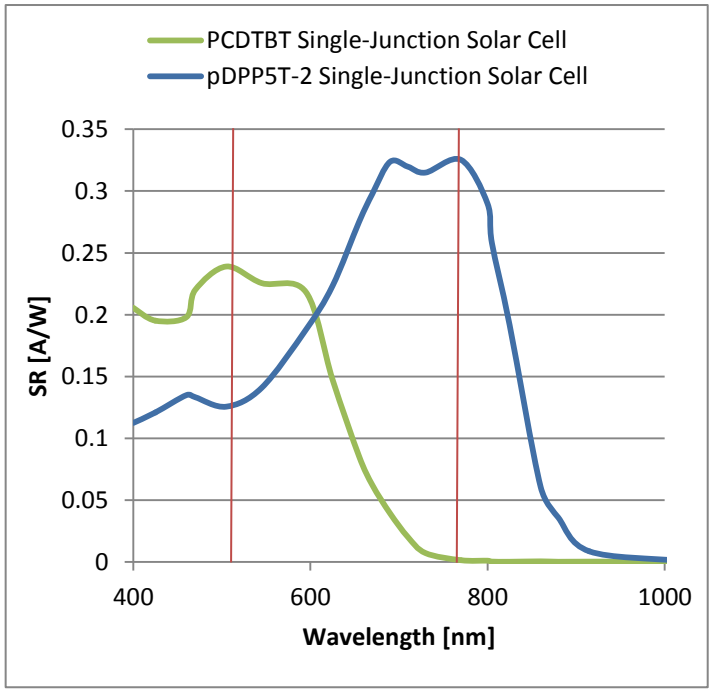


**Figure 6.7:** SR of both single-junction solar cells including the appropriate bias light wavelengths for measuring the tandem solar cell

## 6.2 Spectral Mismatch Correction for Single-Junction Solar Cells

The SR data enable a spectral mismatch correction for the particular solar cells. Neglecting the influence of the mismatch of a solar simulator spectrum can lead to de-optimization of the test cell parameters, like for example layer thickness [38]. A spectral mismatch correction (according to EN 60904-7:2009) is necessary when the test spectrum of a solar simulator differs from the reference spectrum and the SR of the test object differs from the SR of the reference cell. Both conditions are fulfilled at the present case.

The solar simulator is adjusted, such that the reference cell generates the current that it should generate under STC. That does not automatically fulfil the same condition for the test cell. To obtain the short circuit current, a test cell would generate under STC, the measured short circuit current must be divided by the spectral mismatch factor M.

$$I_{TC,STC} = \frac{I_{TC,Sim}}{M} \tag{15}$$

M is calculated according to equation 16.

$$M = \frac{\int E_{Ref}(\lambda) \cdot SR_{Ref}(\lambda)\, d\lambda \cdot \int E_{Sim}(\lambda) \cdot SR_{TC}(\lambda)\, d\lambda}{\int E_{Sim}(\lambda) \cdot SR_{Ref}(\lambda)\, d\lambda \cdot \int E_{Ref}(\lambda) \cdot SR_{TC}(\lambda)\, d\lambda} \tag{16}$$

$SR_{TC}$ = Spectral response of test cell

$SR_{Ref}$ = Spectral response of reference cell

$E_{Sim}$ = Spectrum emitted by simulator

$E_{Ref}$ = Reference spectrum (AM1.5, 1000 W/m²)

Only relative values are required, as constants would minimize. If the test spectrum would perfectly match the reference spectrum or the SR of the test cell is equal to the SR of the reference cell, parts of equation 16 would cancel and M would become 1.

The SR of the reference cell is given by ISE CalLab. The SR data of the cells under investigation are obtained with 80 % monochromatic light intensity and no bias light (chapter 6.1). The calculated spectral mismatch factors are M(PCDTBT) = 1.0539 and M(pDPP5T-2) = 1.0330. That indicates an error of 5.4 % for PCDTBT and 3.3 % for pDPP5T-2, when not applying the spectral mismatch factor.

The reference cell or the test spectrum should be chosen such that $0.98 < M < 1.02$ [39]. This is unfortunately not possible with the solar simulator using the pre-programmed AM 1.5 (1000 W/m²) spectrum.

The composition of the test spectrum AM 1.5 does not influence the results of the SR measurements, as they are conducted with just monochromatic light. Only the data of the I-V-curves need to be corrected.

# 7 Characterisation of Tandem Solar Cells

## 7.1 Influence of Light Intensity on the Spectral Response of the Tandem Solar Cell

**Bias Light Intensity**

To obtain the SR of a tandem solar cell, the sub cell not to be measured has to be biased optically, so it does not limit the current. The optimal wavelengths for bias light in the present case are 505 and 770 nm, as investigated in chapter 6.1.

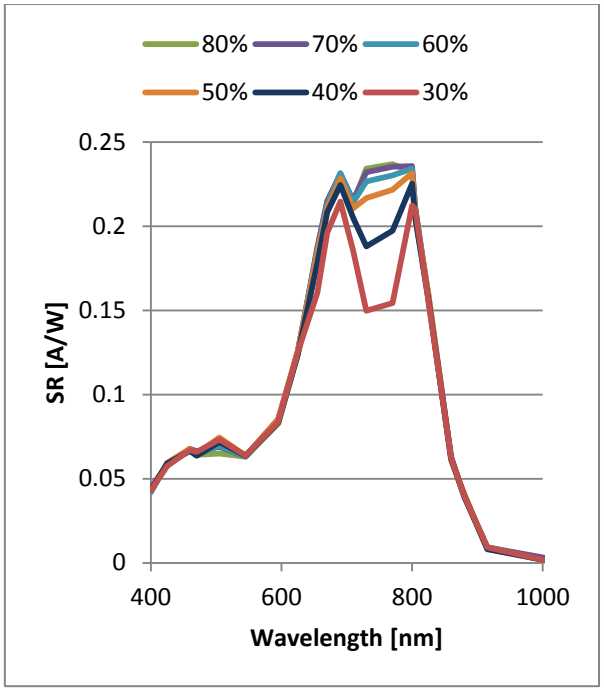


**Figure 7.1:** SR of the tandem solar cell with 505 nm bias light of various intensities (30 – 80 %) and with monochromatic light of 20 % intensity

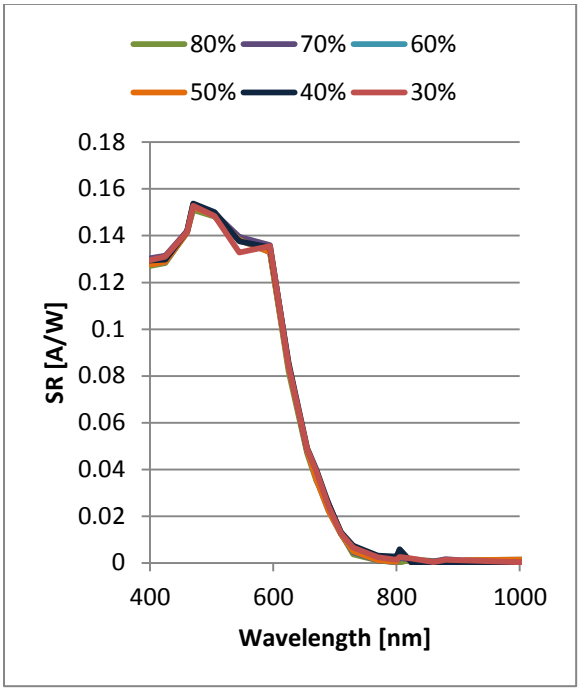


**Figure 7.2:** SR of the tandem solar cell with 770 nm bias light of various intensities (30 – 80 %) and with monochromatic light of 20 % intensity

To flood the optically biased sub cell completely, the intensity of the bias light is chosen to be considerably higher than the intensity of the monochromatic light. In Figure 7.1 and Figure 7.2, the intensity of the bias light is varied from 30 up to 80%, whereas the monochromatic light has a constant intensity of 20 %. In Figure 7.1 bias light with 505 nm and in Figure 7.2 bias light with a wavelength of 770 nm wavelength is used. The SR is calculated according to equation 13.

In Figure 7.1, the signal decreases for low bias light irradiances in the range of maximal absorption, at wavelengths between 690 and 800 nm. The current, generated by the monochromatic light in the sub cell to be measured, exceeds the current generated in the optically biased sub cell. At a wavelength of 505 nm, slight deviations are recognized. Those can be traced back to inaccuracies in calibration when providing monochromatic and bias light of the same wavelength.

For the second sub cell, as graphed in Figure 7.2, the measurement artefacts are less markedly. Only a slight decrease can be realized at a wavelength of 545 nm. This effect occurs due to the enhanced irradiance of the 545 nm LED group compared to the other LED groups at the same intensity, as shown in Figure 5.2.

**Monochromatic Light Intensity**

The intensity of the monochromatic light influences the results as well. In Figure 7.3, the SR of both sub cells in the tandem are shown with a monochromatic light of 30 % intensity and a bias light of 70 % intensity.

The SR in Figure 7.3 is increased compared to Figure 7.1 and Figure 7.2, where the monochromatic light intensity is only 20 %. However, when using 30 % intensity of the LEDs for monochromatic light, the bias light intensity cannot exceed 70 %. When using a bias light of 505 nm, the SR drops at wavelengths between 690 and 800 nm. This is the range where the current of the sub cell to be measured gets maximal and exceeds the current of the optically biased sub cell. The current is limited by the optically biased sub cell and thus the SR obtained is lower than the actual value.

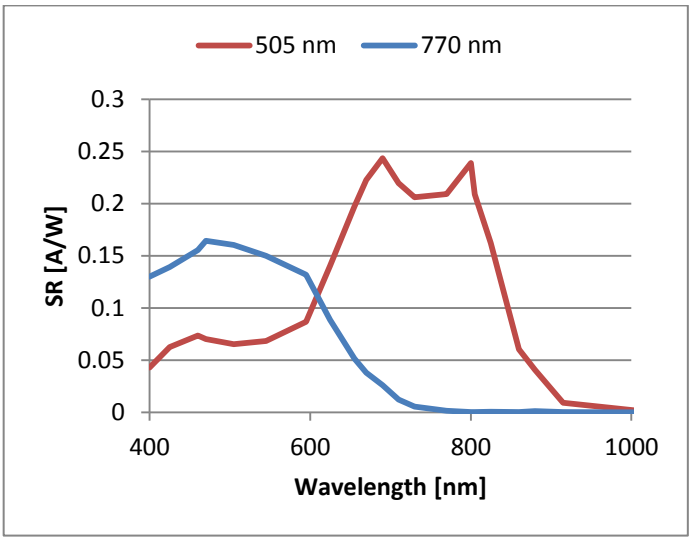


**Figure 7.3:** SR of the tandem solar cell with bias light of 70 % intensity and with monochromatic light of 30 % intensity

In Figure 7.4 and Figure 7.5 a monochromatic light intensity of 10 % is used. The SR is shown, depending on the intensity of the bias light.

When a low monochromatic light intensity of 10 % is chosen, the optically biased sub cell already generates a high enough current, using a bias light intensity of 30 %. Further increase of bias light intensity does not influence the SR curve. For all intensities of bias light used, the bias current exceeds the current generated by the monochromatic light. Hence, the sub cell to be measured is current limiting for all wavelengths. However, for a monochromatic light of 10 % intensity, a drop in the SR curve compared to higher monochromatic light intensities can be observed. The SR values at the absorption maxima are about 0.5 A/W lower than in Figure 7.3, where the monochromatic light intensity is 30 %.

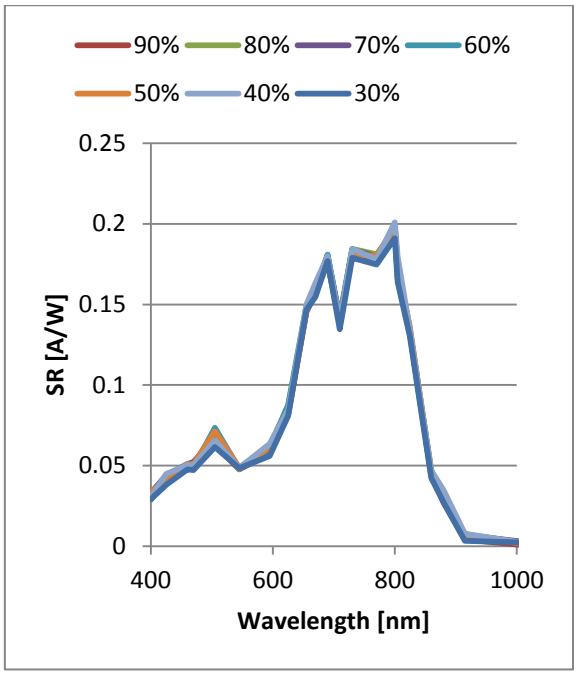


**Figure 7.4:** SR of the tandem solar cell with 505 nm bias light of various intensities (30 – 90 %) and with monochromatic light of 10 % intensity

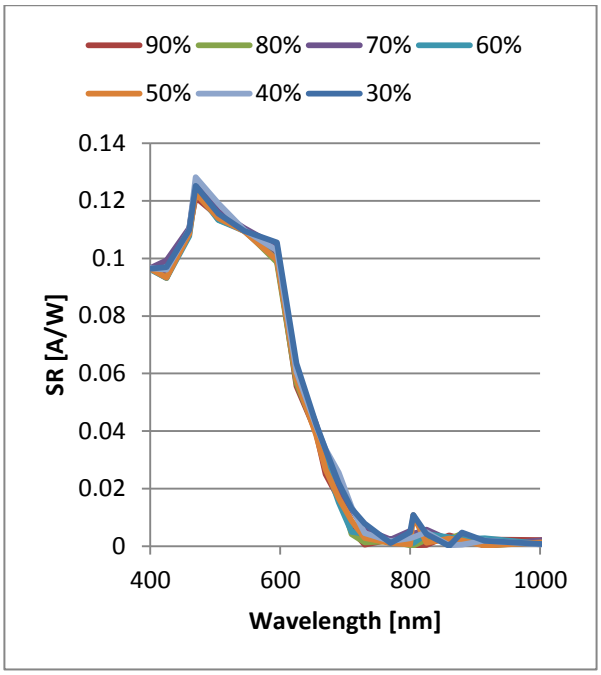


**Figure 7.5:** SR of the tandem solar cell with 770 nm bias light of various intensities (30 – 90 %) and with monochromatic light of 10 % intensity

Hence, a compromise regarding the adjustment of the light intensities is found for the following measurements. The monochromatic light is adjusted to an intensity of 20 % and the bias light to 80 %.

## 7.2 Influence of the Bias Voltage on the Spectral Response of the Tandem Solar Cell

To obtain the correct SR of one sub cell, it has to be measured in short circuit. When measuring a tandem solar cell in short circuit, the sub cell to be measured is usually operating at a reverse bias voltage. This fact is described in chapter 3.3. To measure the required sub cell in short circuit, a bias voltage in the magnitude of the $V_{OC}$ of the optically biased sub cell must be applied to the tandem solar cell. The $V_{OC}$ is obtained by using the I-V-characteristics of the single-junction solar cells. The bias voltage is applied with the SMU. Instead of measuring at 0 V, the required value of voltage is inserted in the software.

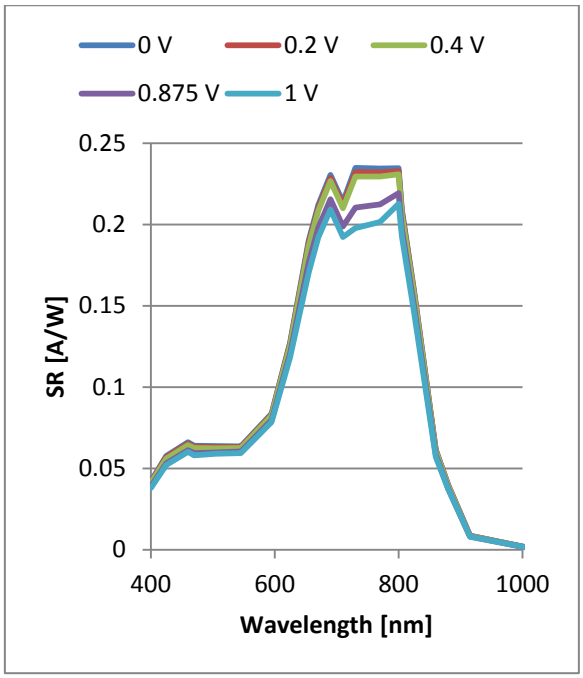


**Figure 7.6:** SR of the tandem solar cell with 505 nm bias light of 80 % intensity and with monochromatic light of 20 % intensity depending on the bias voltage

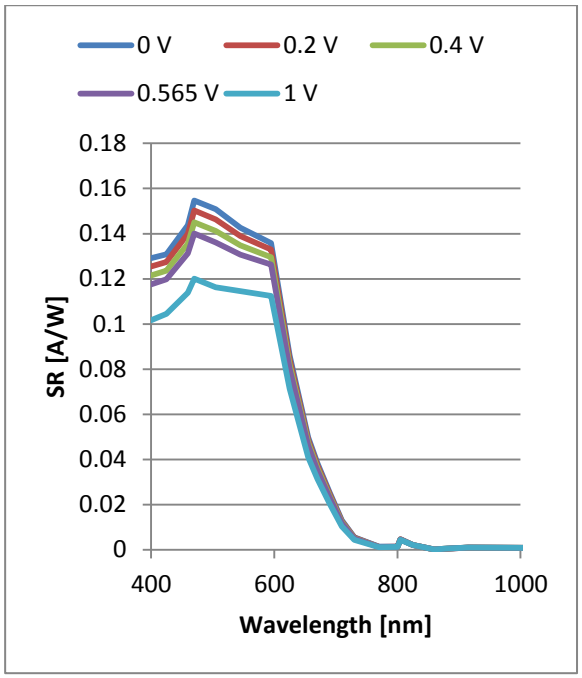


**Figure 7.7:** SR of the tandem solar cell with 770 nm bias light of 80 % intensity and with monochromatic light of 20 % intensity depending on the bias voltage

The bias voltage measurements are performed with monochromatic light of 20 % and bias light of 80 % intensity, as these conditions showed the best results in previous tests.

In Figure 7.6 and Figure 7.7, the influence of various forward bias voltages between 0 and 1 V on the SR of the tandem solar cell is represented. To be measured in short circuit, for the pDPP5T-2 sub cell a bias voltage of 0.975 V and for the PCDTBT sub cell a bias voltage of 0.565 V is required.

As already explained in [18], the curves just change their absolute height and relative changes in wavelength are minor. The lower the bias voltage, the higher is the SR curve due to the larger space charge width. [31]

## 7.3 S-Shape of the Tandem Solar Cell and Treatment with UV Light

When measuring the sub cells of a tandem solar cell under application of bias voltage, the I-V-characteristic of the tandem solar cell has to be taken into account. For degraded organic tandem solar cells, the I-V-curve under illumination exhibits an s-shape. This s-shape is strengthened with increasing age of the cell. The dark I-V-curve shows no such behaviour. Figure 7.8 represents the I-V-curve for different states of degradation of the organic tandem solar cell.

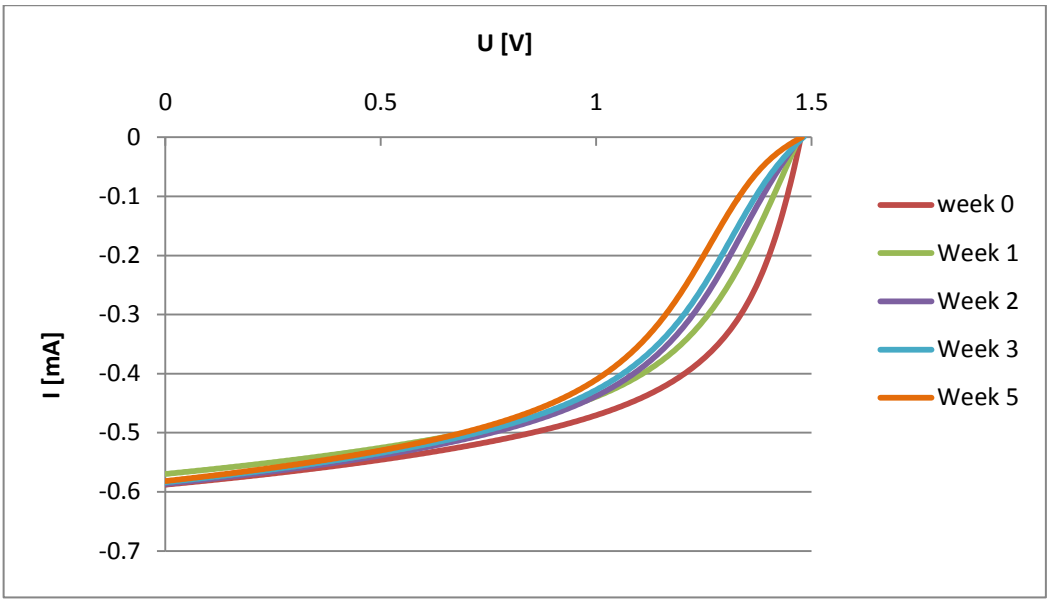


**Figure 7.8:** Change of the I-V-curve due to degradation of the tandem solar cell

The intermediate layer of the organic tandem solar cell consists of two components, ZnO and PEDOT:PSS. The s-shape expresses a bad ohmic contact between ZnO and PEDOT:PSS, which acts as p-n-junction and thus as counter-diode. This causes a voltage drop, resulting in an s-shaped I-V-curve [40], in combination with reduction of $R_S$, $R_{SH}$ and FF. The s-shape can be eliminated by doping of ZnO and PEDOT:PSS. As PEDOT:PSS is already heavily p-doped, doping has to be applied to ZnO. This is done by UV radiation [41, 42]. The UV radiation causes an enhancement of free carrier concentration [43]. Exposure of the organic tandem solar cell to only a few seconds of UV irradiation is sufficient to eliminate the s-shape. Due to the increased conductivity of ZnO after UV irradiation, the $V_{OC}$ and $I_{SC}$ can also be increased [40]. Improvements in $R_S$, $R_{SH}$ and FF can also be recognized after exposure to UV radiation. In Figure 7.9, Figure 7.11 and Figure 7.13 the $R_S$, $R_{SH}$ and fill factor (FF) depending on the state of degradation are shown. Figure 7.10, Figure 7.12 and Figure 7.14 demonstrates the $R_S$, $R_{SH}$ and FF for the same organic tandem solar cell after UV-treatment. The five curves in the diagram represent five of the six cells on the substrate of the inverted organic tandem solar cell under test. The contact to cell 5 is damaged. Thus it is not shown in the diagrams.

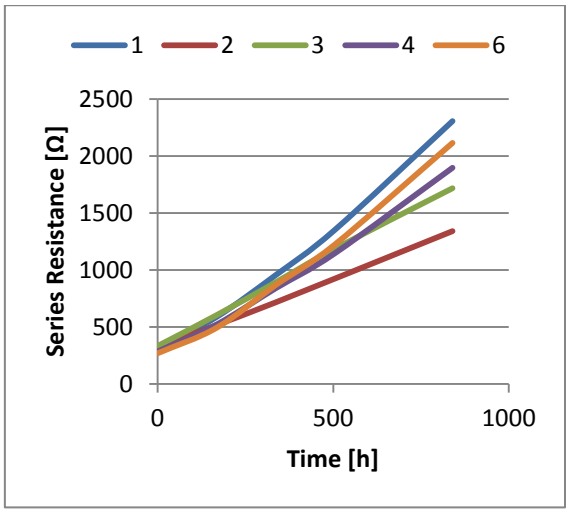


**Figure 7.9:** Series resistance of tandem solar cell before exposure to UV radiation

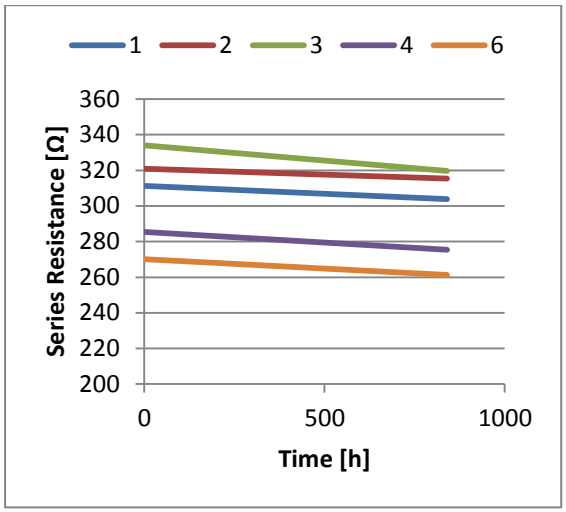


**Figure 7.10:** Series resistance of tandem solar cell after exposure to UV radiation

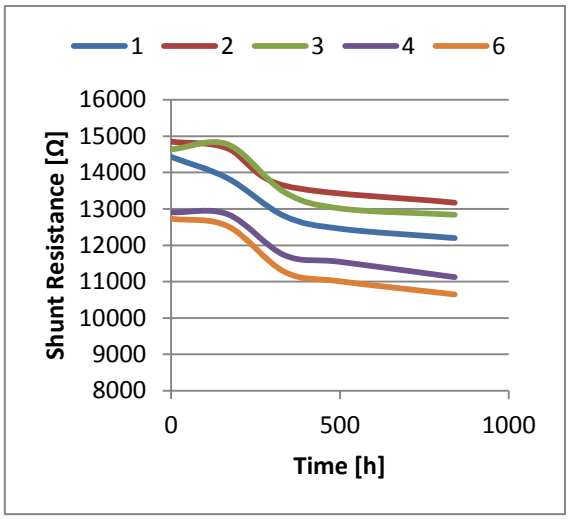


**Figure 7.11:** Shunt resistance of tandem solar cell before exposure to UV radiation

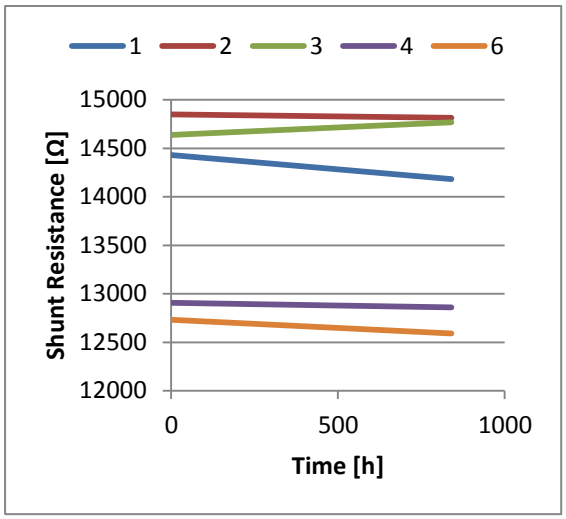


**Figure 7.12:** Shunt resistance of tandem solar cell after exposure to UV radiation

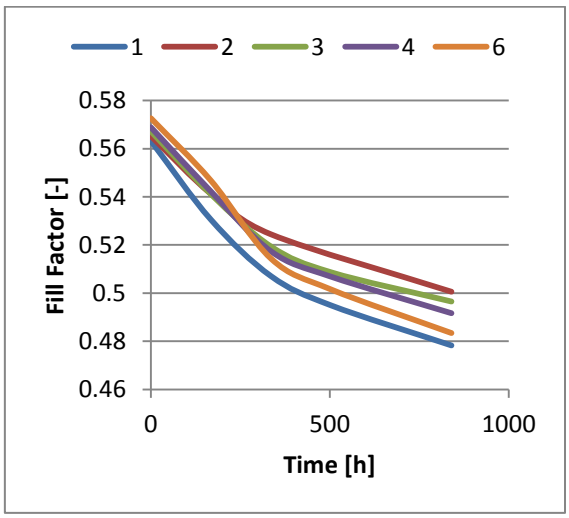


**Figure 7.13:** Fill factor of tandem solar cell before exposure to UV radiation

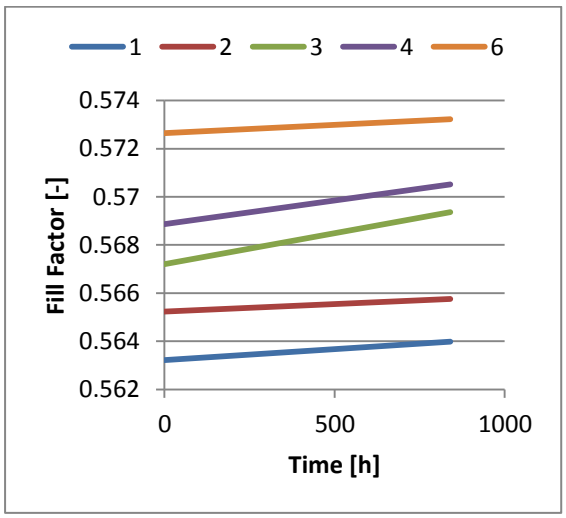


**Figure 7.14:** Fill factor of tandem solar cell after exposure to UV radiation

When exposing the tandem solar cell to UV-light, despite of its age (840 h, 5 weeks) it shows better values for its parameters than in the beginning. The series resistance is decreased, whereas the shunt resistance and the FF are enhanced by UV treatment.

Figure 7.15 shows the I-V-curve of the same tandem solar cell before and after exposure to UV-light.

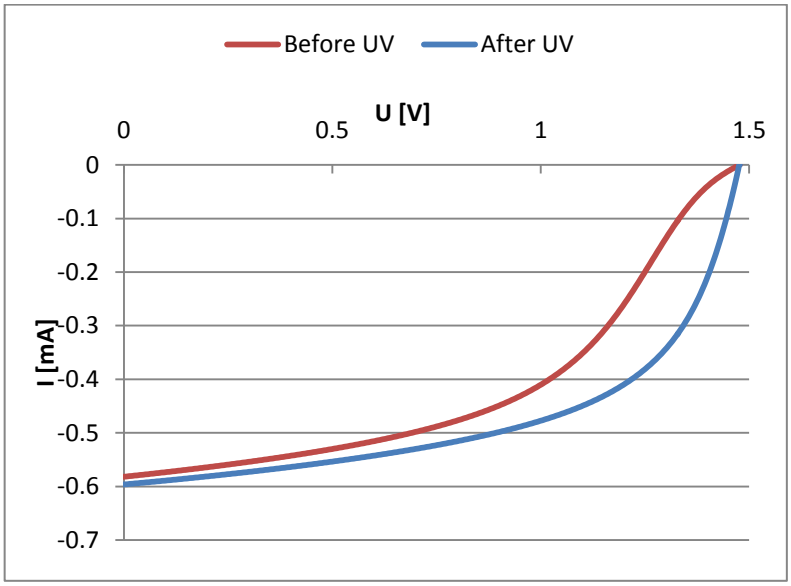


**Figure 7.15:** I-V-curve of the organic tandem solar cell before and after exposure to UV radiation

The signs of degradation can be completely reversed by the UV radiation. When applying bias voltage at SR measurements, the measuring point is shifted in forward bias direction. When the solar cell is degraded, the SR measured is decreased in comparison to the actual value. Thus it is important to expose the organic tandem solar cell to UV light before SR measurement.

## 7.4 Spectral Mismatch Correction for Tandem Solar Cells

For testing the illuminated I-V-curve of a tandem solar cell with a solar simulator, to obtain STC, a spectral mismatch correction has to be applied as well. The characteristics of multi-junction solar cells are very sensitive to the spectral distribution of the incident irradiation. Unfortunately, there is no simple calculation of the spectral mismatch correction available for tandem solar cells [44]. Unlike in single-junction solar cells, the spectral mismatch factor depends not only on the SR of the front and rears cell and the spectrum emitted by the solar simulator, but also on the blocking ability of the limiting junction [44].

Fraunhofer ISE [18, 45] provides a measure for calculating the required intensities of a multisource solar simulator, to fulfil STC for a multi-junction solar cell. This approach is described for tandem solar cells hereinafter. The aim is to adjust the simulator spectrum, such that each sub cell generates the same photo-current than it would under the reference spectrum. In equation 17, the photo-current generated by each sub cell under the desired reference spectrum $E_{ref}(\lambda)$ (e.g. AM 1.5) is calculated.

$$J_{ref,i,j} = \int SR_{i,j}(\lambda) \cdot E_{ref}(\lambda) d\lambda = C_{i,j} \cdot \int sr_{i,j}(\lambda) \cdot E_{ref}(\lambda) d\lambda \quad (17)$$

$SR_{i,j}(\lambda)$ = absolute SR of each sub cell i,j

$sr_{i,j}(\lambda)$ = relative SR of each sub cell i,j

$C_{i,j} = \frac{SR_{i,j}(\lambda)}{sr_{i,j}(\lambda)}$ = ratio of the absolute to the relative SR, independent on wavelength

As in practical applications only the lower of both photo-currents will flow, in this case $J_{ref,i/j}$ is interpreted as the charge carrier generation and not as external current.

Equation 18 gives the generated photo-current density under the spectrum of the solar simulator with two light sources.

$$J_{sim,i,j} = C_{i,j} \cdot A_1 \int sr_{i,j}(\lambda) \cdot e_1(\lambda) d\lambda + C_{i,j} \cdot A_2 \int sr_{i,j}(\lambda) \cdot e_2(\lambda) d\lambda \quad (18)$$

$e_{1,2}(\lambda)$ = relative spectra of the two light sources

$A_{1,2}$ = intensity factors of the two light sources

For the calibration of the solar simulator, the photo-current density under the simulator spectrum has to match the current density under the reference spectrum. The following linear equation system is obtained. The factors $C_{i,j}$ cancel out. The equations can be resolved into $A_1$ and $A_2$.

$$A_1 \int sr_{i,j}(\lambda) \cdot e_1(\lambda) d\lambda + A_2 \int sr_{i,j}(\lambda) \cdot e_2(\lambda) d\lambda = \int sr_{i,j}(\lambda) \cdot E_{ref}(\lambda) d\lambda \quad (19)$$

For adjusting the light sources of the solar simulator, a reference cell is used, which covers the range of SR of each sub cell. In equation 20 the photo-current density, the reference cell would generate under test light conditions ($A_1$, $A_2$, $e_1$, $e_2$), is calculated.

$$J_{E_{1,2},RC} = A_{1,2} \cdot \int SR_{RC}(\lambda) \cdot e_{1,2}(\lambda) d\lambda \quad (20)$$

$SR_{RC}(\lambda)$ = absolute spectral response of the reference cell

The solar simulator is adjusted, until the generated photo-currents meet the value of the calculated photo-currents. This is not applicable in the present setup as the light intensities are already tuned to their maximum. But the intensities to be applied can be estimated with the following approximations.

The first light source is represented by the pre-programmed test spectrum (AM 1.5, 1000 W/m²). Two possibilities are tried for the second light source, quasi-monochromatic light with 505 and 770 nm at 80 % intensity, like used as bias light in former measurements.

The photo-current densities, generated by both light sources, were measured separately and compared with the calculated photo-current densities from equation 18. The ratio of both photo-current densities roughly gives the tuning factor in order to observe STC. For the calculations, linearity of the solar cell is assumed. The test spectrum between 900 and 1050 nm cannot be recorded and thus is assumed to correspond to the reference spectrum. Anyway, the spectrum in this range does not count much weight, as the SR of the test devices at these wavelengths is very low.

The tuning-factor for the pre-programmed AM1.5 (1000 W/m²) spectrum would be 0.909 under usage of quasi-monochromatic light of 770 nm of 17.142 % intensity (=7.02 W/m²) as second light source. Quasi-monochromatic light of 505 nm is not applicable as second light source, as the linear equation system (equation 19) cannot be solved. In practical, a decrease of the spectrum at 505 nm is necessary in order to obtain a suitable test spectrum.

## 7.5 Dark Spectral Response and White-Biased Spectral Response of the Tandem Solar Cell

Additional information can be obtained by the dark SR and the SR with white bias light. Figure 7.16 shows the SR curves for bias lights of 505 and 770 nm and additionally the dark SR curve, where the cell is measured with only monochromatic radiation. Figure 7.17 represents additionally the SR curve with white bias light applied instead of bias light of only one wavelength.

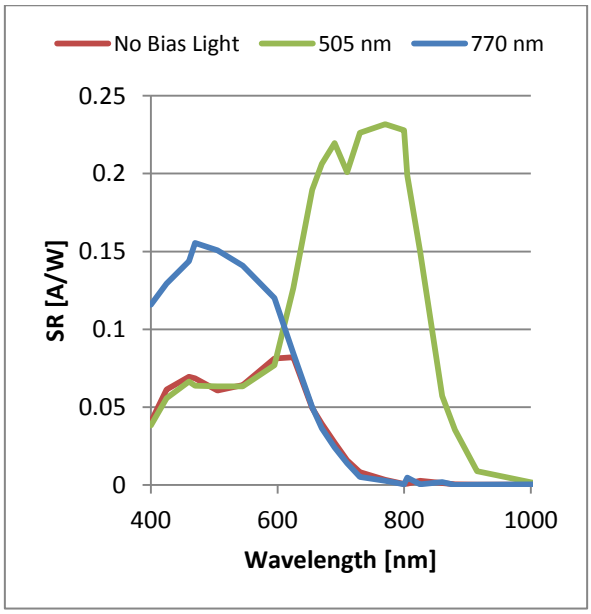


**Figure 7.16:** SR of the tandem solar cell with bias light of 505 and 770 nm and additionally without bias light

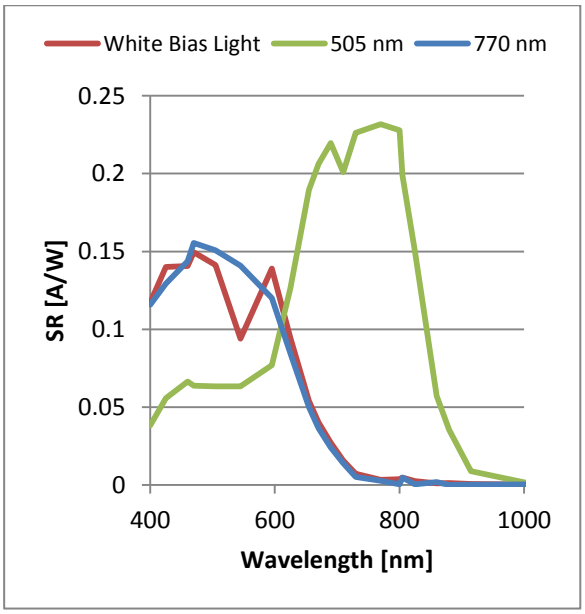


**Figure 7.17:** SR of the tandem solar cell with bias light of 505 and 770 nm and additionally with white bias light

The dark SR curve always corresponds to the lower SR of the both sub cells at each wavelength. Only the photons that are absorbed in both sub cells, contribute to the dark SR curve.

The SR curve with white bias light should be equal to the curve of the power-limiting sub cell. The PCDTBT sub cell is proven to be power-limiting. The application of white bias light is not suitable when measuring the SR with the LED solar simulator. The SR curve is distorted due to white bias light, like the curves in chapter 6.1. Remarkable is the kink at 545 nm, due to the high irradiance of the LED group at this wavelength. Calibration errors result by the application of two light sources with one LED group.

## 7.6 Influence of the Shunt Resistance on the Spectral Response of the Tandem Solar Cell

Besides fulfilling the condition to measure the sub cell under investigation in short circuit, the bias voltage is also used to minimize measuring artefacts due to a low $R_{SH}$. Measuring artefacts are characterized by an increased SR in the range, where the other sub cell does absorb, and simultaneously decrease of SR in the actual absorption range of the measured sub cell.

The following tests show the influence of the $R_{SH}$ on the SR. For those tests, the hand-made silicon tandem solar cell from Figure 4.8 is used. The cells have a low shunt resistance, when not previously isolating the edge. To increase the shunt resistance the edges are filed off in several steps. The sub cell with the varied $R_{SH}$ is equipped with the black filter (bandpass-filter with central wavelength at 830 nm), while the other sub cell with a constant $R_{SH}$ of 1160 Ω is equipped with a blue filter (bandpass-filter with central wavelength at 507 nm). Figure 7.18 and Figure 7.19 show the SR of the sub cell with varied $R_{SH}$ in a tandem compound, when biased with 505 nm. The SR of the sub cell with the blue filter is represented in Figure 7.20 and Figure 7.21.

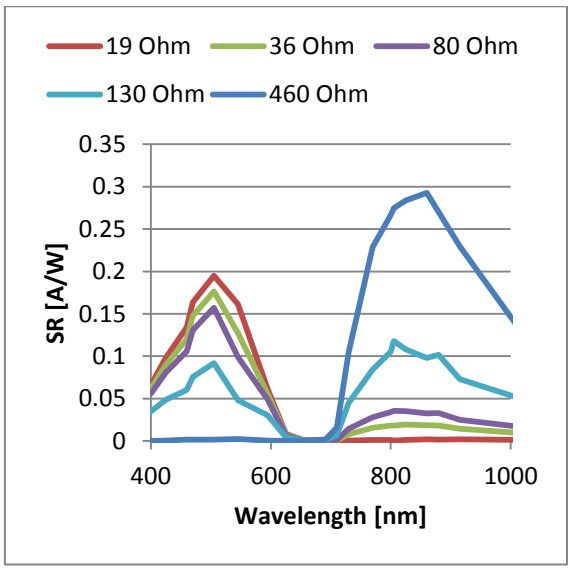


**Figure 7.18:** Tandem solar cell measured with bias light of 505 nm under variation of the $R_{SH}$ of the black filtered sub cell without application of bias voltage

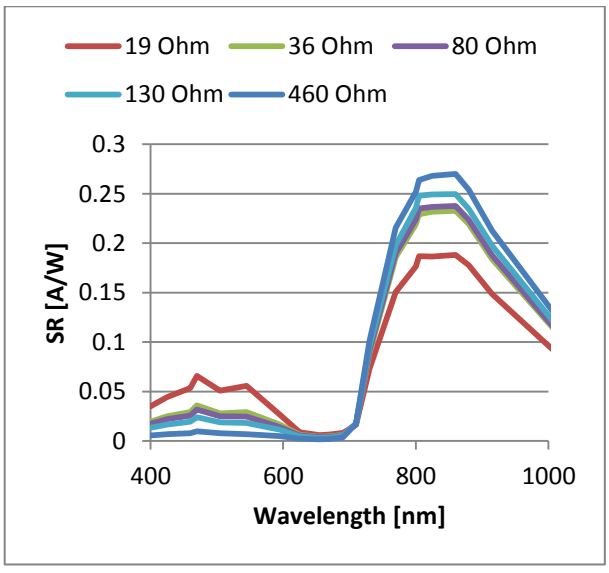


**Figure 7.19:** Tandem solar cell measured with bias light of 505 nm under variation of the $R_{SH}$ of the black filtered sub cell with bias voltage applied

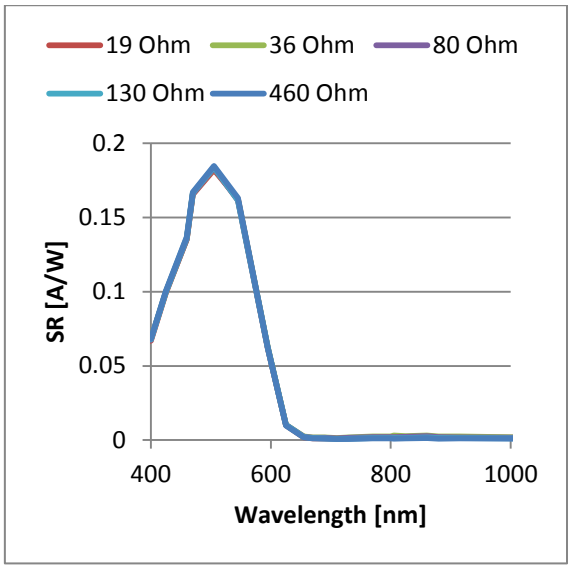


**Figure 7.20:** Tandem solar cell measured with bias light of 860 nm under variation of the $R_{SH}$ of the black filtered sub cell without application of bias voltage

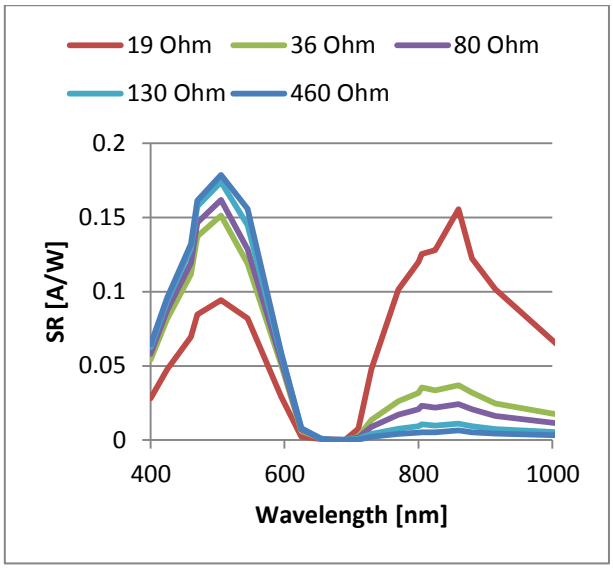


**Figure 7.21:** Tandem solar cell measured with bias light of 860 nm under variation of the $R_{SH}$ of the black filtered sub cell with bias voltage applied

The $R_S$ is kept constant at 0.7 Ω during the following measurements.

The values of $R_S$ and $R_{SH}$ are obtained from the illuminated I-V-curve with the help of a program, developed in previous studies on the ZAE.

To measure the sub cell with the black filter in a tandem, it must be current limiting. However, when the current can flow over a low $R_{SH}$, this specific sub cell cannot be current-limiting and instead the SR of the other sub cell is measured. The measuring artefacts in Figure 7.18 can be explained by the following considerations.

**Low RSH (19 Ω)**

The current generated by the bias light ($I_{bias}$) is very high, due to not being limited by the $R_{SH}$ of the sub cell with the black filter. The current, generated by the sub cell with the black filter, is much lower than $I_{bias}$. Additionally, a high share of the current, generated in the black filtered sub cell, flows back over its own shunt resistance [46]. In the absorption range of the optically biased sub cell, additional current is generated by the monochromatic light, which is not limited by the sub cell with the black filter. Even though $I_{bias}$ is subtracted to obtain the SR, a high current can be measured in the absorption range of the optically biased sub cell.

**Middle $R_{SH}$ (36 Ω, 80 Ω, 130 Ω)**

$I_{bias}$ is slightly limited by the increased $R_{SH}$. The current generated in the black-filtered sub cell by monochromatic light ($I_{mono}$) already contributes significantly to the total current. But still, in the absorption range of the blue-filtered sub cell, an increased current can be measured. However, the current, generated by

the sub cell with the blue filter, is slightly limited by the $R_{SH}$ of the other sub cell. The limitation increases, the higher the $R_{SH}$ of the sub cell with the black filter is.

**High RSH (460Ω)**

$I_{bias}$ is strongly limited by the $R_{SH}$ of the black filtered sub cell. The current, additionally generated by monochromatic light in the blue filtered sub cell, is also namely limited by the $R_{SH}$ of the sub cell with black filter. Thus, no SR is measured in the absorption range of the blue filtered sub cell. Only in the absorption range of the black-filtered sub cell, a current can flow. The sub cell with the black filter is current-limiting for all wavelengths.

The SR of the black filtered cell is also measured separately. The SR of the single-junction solar cell appears to be not influenced by the $R_{SH}$. Thus, the current generated in the black filtered sub cell in the tandem compound is independent of its $R_{SH}$ value.

When applying no bias voltage, the SR of the blue filtered sub cell is independent of the $R_{SH}$ of the black filtered sub cell. The blue filtered sub cell's current-limiting ability is not influenced by the $R_{SH}$ of the black filtered sub cell. Only the SR of the sub cell with the low $R_{SH}$ is influenced, as its blocking ability changes. When applying bias voltage, both SR curves are influenced. The lower the $R_{SH}$ of the black filtered sub cell, the more distorted get the SR curves. However, the influence is only significant at a very low $R_{SH}$ (in this case 19 Ω). Hence, when measuring the tandem solar cell with bias voltage, the error can be reduced. A reason for the distortions of the SR in Figure 7.19 can be the blue filtered sub cell not operating close to its $V_{OC}$ when optically biased, due to the current, flowing over the low $R_{SH}$ of the black filtered sub cell. Thus, the magnitude of the bias voltage is not chosen appropriately.

The bias voltage can be tuned either to minimize measuring artefacts, or to keep the sub cell under investigation in short circuit. Both conditions can mostly not be combined at the same bias voltage [46]. The bias voltage appropriate to reduce measuring artefacts is not further investigated. The focus is set on measuring the object in short circuit.

The $R_{SH}$ of the organic tandem solar cell under investigation is over $10^4$ Ohm. Thus, the measurement results are not influenced by the $R_{SH}$.

## 7.7 Influence of the Series Resistance on the Spectral Response of the Tandem Solar Cell

The influence of the series resistance on the measurement of the SR can be derived from the equivalent circuit of a tandem solar cell. In Figure 7.22, the equivalent circuit is shown without application and in Figure 7.23 with application of bias voltage in the appropriate magnitude.

Usually, the bias voltage is chosen in the magnitude of the open circuit voltage of the optically biased sub cell. Anyway, a huge series resistance can influence the magnitude of the appropriate bias voltage.

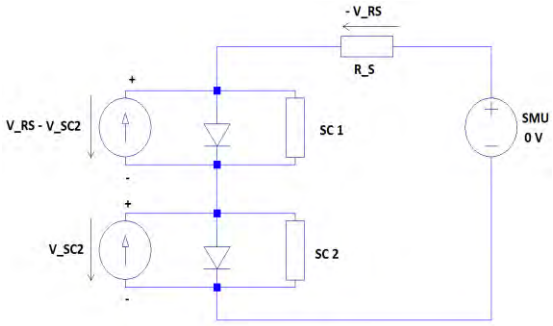


**Figure 7.22:** Equivalent circuit of a tandem solar cell used for determining the influence of the series resistance without applying bias voltage

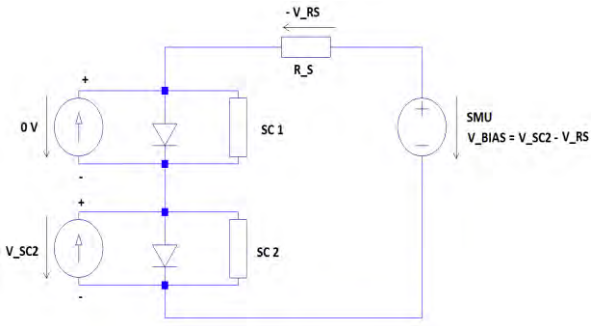


**Figure 7.23:** Equivalent circuit of a tandem solar cell used for determining the influence of the series resistance under application of bias voltage

In the following considerations the bias voltage is adjusted, to measure the SR of the tandem solar cell without additional series resistance (0 Ω). The tandem solar cell itself has a series resistance of 0.7 Ω, which is considered as negligible. Subsequently, a resistance of 270 Ω is switched in series to the tandem solar cell. 270 Ω is the magnitude of the series resistance of the organic tandem solar cell tested in chapter 7. The SR curves for both sub cells are represented in Figure 7.24 and Figure 7.25. With an enhancement of the series resistance, distortions of the SR are recognized. The bias voltage, appropriate for a tandem solar cell with 0 Ω series resistance, is too high for a sample with a series resistance of 270 Ω. As shown in Figure 7.23, the bias voltage should have the magnitude of the open circuit voltage of the optically biased sub cell, minus the voltage drop over the series resistance. This proposition is hard to realize, as for each wavelength of monochromatic light, another current is generated, thus a different voltage drops over the series resistance. Hence, the SR curve for a high series resistance is not just reduced, but also its shape is distorted.

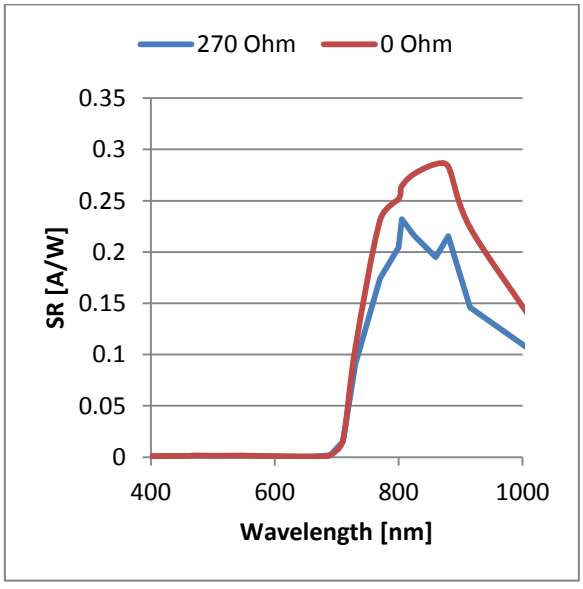


**Figure 7.24:** SR of the tandem solar cell with bias light of 505 nm and application of bias voltage for two different magnitudes of series resistance

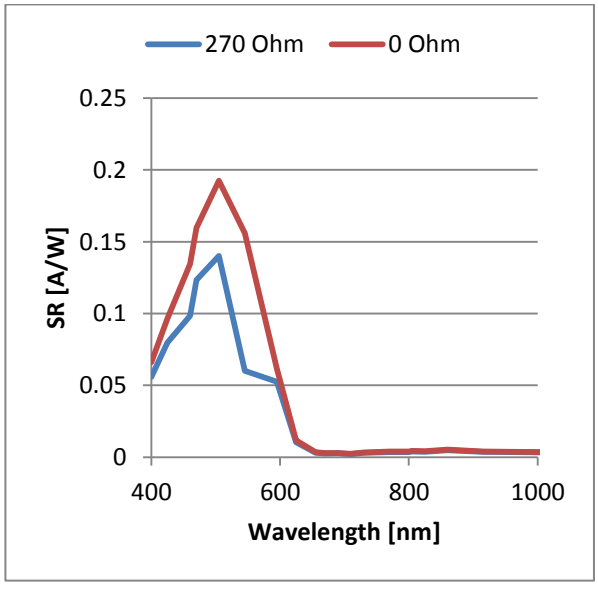


**Figure 7.25:** SR of the tandem solar cell biased with bias light of 860 nm and application of bias voltage for two different magnitudes of series resistance

The series resistance does not only affect the SR of the tandem solar cell, but also the SR of the single junction solar cell. For a huge series resistance, the solar cell is not measured in short circuit, as intended to,

but at a voltage of the magnitude of the voltage drop over the series resistance. Figure 7.26 and Figure 7.27 show the SR of both single junction solar cells, for monochromatic light intensities of 20 and 80 % for two different magnitudes of series resistance (0 Ω, 270 Ω).

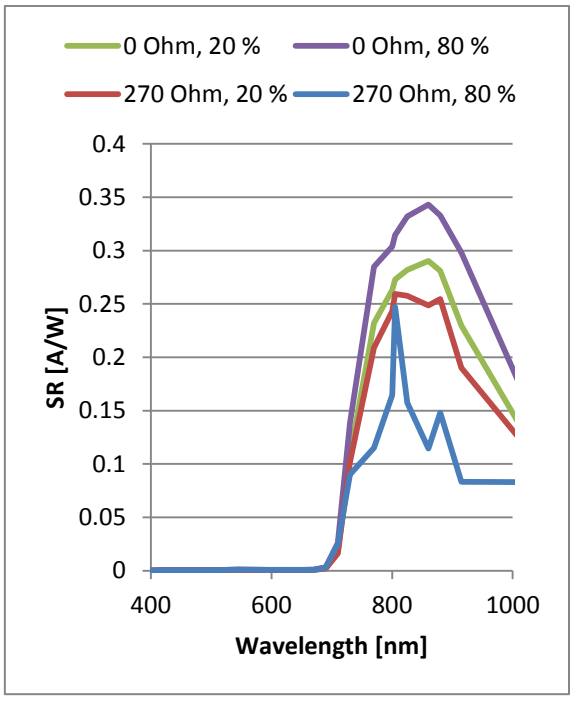


**Figure 7.26:** Influence of the series resistance on the SR of the black filtered single-junction depending on the monochromatic light intensity

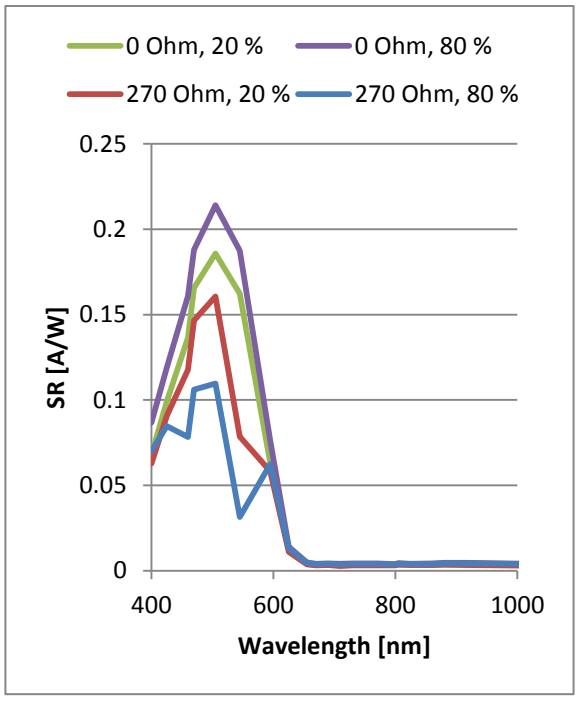


**Figure 7.27:** Influence of the series resistance on the SR of the blue filtered single-junction depending on the monochromatic light intensity

A higher light intensity leads to a higher current generation in the solar cell. For a significant high series resistance, the voltage drop, and thus the measurement artefacts increase. The influences of the series resistance are lower, when a lower current is flowing. Thus, the SR of the solar cell with high series resistance is not as distorted, when measured with a monochromatic light intensity of 20 %, compared to 80 %.

Anyway, for the organic solar cell, tested in chapter 6 and 7, the effect of the series resistance is not significant. The maximum current generated by the organic tandem solar cell in SR measurements is $6 \cdot 10^{-5}\ A$. For a series resistance of about 300 Ω, the resulting voltages drop is 0.018 V. In comparison, in the silicon tandem solar cell the maximum current in SR measurements is $2.7 \cdot 10^{-3}$ A. In this case, the voltage dropping over a 270 Ω series resistance is 0.73 V. The error due to the series resistance, when measuring organic solar cells, is considered as negligible.

To not influence the measuring result significantly, the series resistance must be lower, the higher the current generated in the solar cell is. It could not be taken a final statement about the value of the series resistance allowed.

## 7.8 Comparison to Data from another Measuring Arrangement

**Comparison to the Measuring Arrangement at KIT**

The organic solar cells from KIT are measured with the LED solar simulator under the same conditions like the organic solar cells from I-Meet. For the single-junction solar cells, a monochromatic light of 80 % intensity is used. The tandem solar cells are measured with bias light intensity of 80 % and monochromatic light intensity of 20 %. The SR curves, obtained from the measuring results, are compared to the data measured at KIT.

At KIT, the single-junction solar cells were measured with white bias light provided by a solar simulator (Oriel Instruments / Newport Corporation). The light was focused on the sample by mirrors. Additionally, the light of a Xe lamp was chopped and coupled into a monochromator. For measuring the tandem solar cells, the bias light, however, was provided by an LED panel, whose intensity was tuned up until the current signal of the tandem solar cell remained constant. Three wavelengths of bias light were possible: 470 nm, 700 nm and 780 nm. No statements were made about the irradiation of either light source.

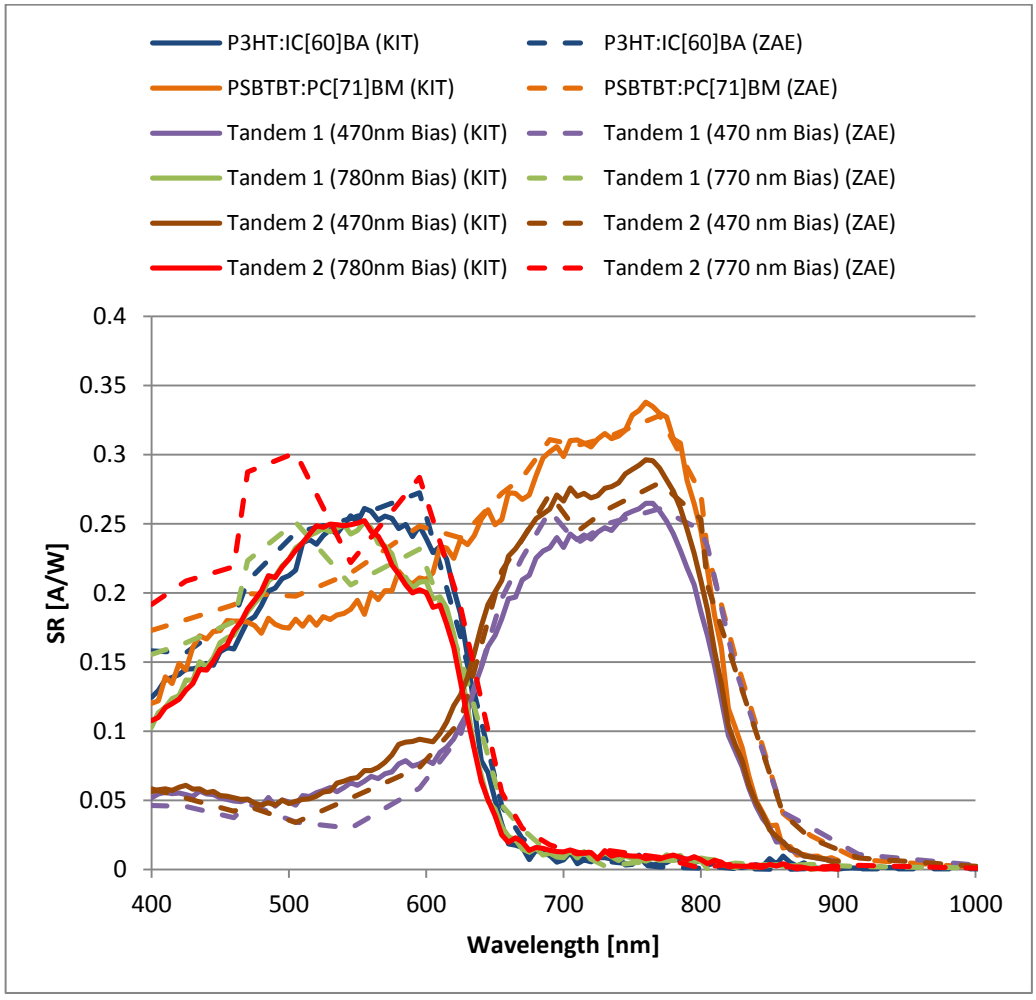


**Figure 7.28:** SR of two tandem solar cells and their respective single-junction solar cells measured with the LED solar simulator and an SR measuring arrangement at KIT

The bias light wavelengths, used at KIT for measuring the SR of the tandem solar cell, were 470 nm and 780 nm. As in the present measuring arrangement no LED group with 780 nm is available, 770 nm is taken as bias light. For comparison purposes, 470 nm is also used as bias light, even though at the LED solar simulator there are more appropriate wavelengths for bias light available, like for example 545 nm. For all tandem solar cell measurements appropriate bias voltage was applied.

Figure 7.28 represents the results of both measuring arrangements and indicates the wavelengths used as bias light. The SR of the single-junction solar cells, measured with the LED solar simulator, strongly correlate with the results from KIT. Just in the lower wavelength range an enhancement of the SR, measured with the LED solar simulator, can be recognized. The SR curves of the tandem solar cells, when biased with 470 nm, also match the curves from KIT. Only the curves of the tandem solar cell, when biased with 770 nm, deviate from the comparative values. One reason can be the different bias light wavelength. Also the fact, that the SR measured with the LED solar simulator is enhanced in the low wavelength range, can contribute to this deviation.

The SR curves of the tandem solar cells, when biased with 770 nm, show a kink at 545 nm. Varying the intensities of monochromatic and bias light does not lead to elimination of the kink at 545 nm. No proper explanation is found. Subsuming, the SR of both measuring arrangements strongly correlate.

**Comparison to the Measuring Arrangement at I-Meet**

The organic tandem solar cell from I-Meet is also measured at the SR and measuring arrangement at I-Meet for comparison purposes.

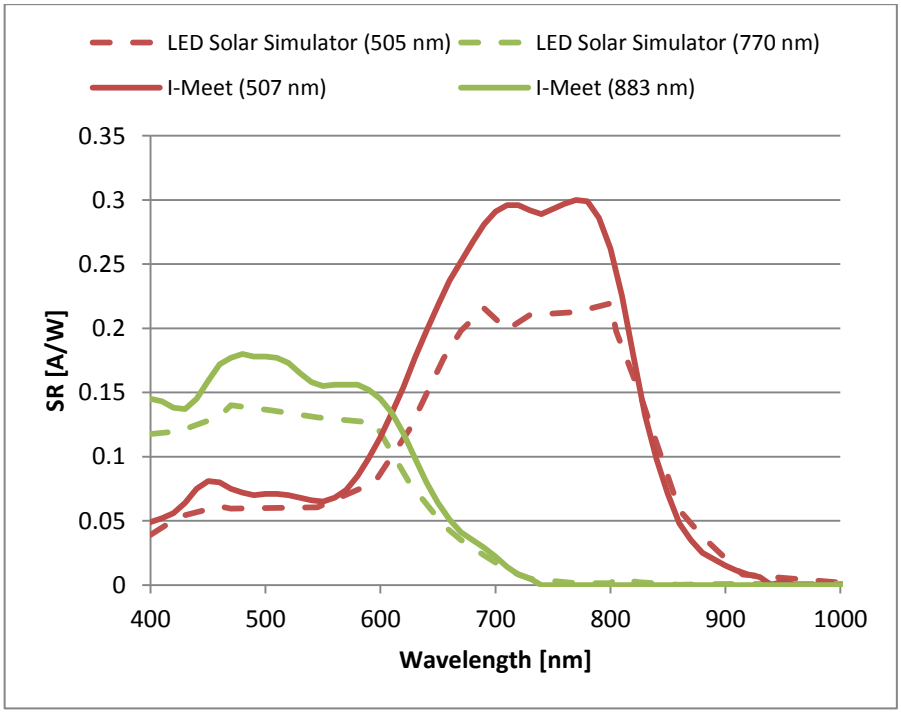


**Figure 7.29:** Comparison measurements taken at the SR measuring arrangement at I-Meet with the same bias voltage and bias light wavelengths as with the LED solar simulator

At I-Meet, there is an accredited (according to ISO/IEC 17025 (TAF)) measuring arrangement (Enlitech QE-R) for SR and EQE available. In this measuring arrangement, a 150 W XQ lamp provides continuous light of about 300 – 200 nm. This light is monochromatized and chopped. The signal is recorded with the help of a lock-in amplifier. For the white bias light, a 150 W Xenon (Xe) and Quarz Tungsten Halogen (QTH) dual-lamp source is available with different filters. Thus, also monochromatic bias light can be provided. For the present measurement, the light sources are tuned to their maximum.

For both measurements, with the LED solar simulator and the accredited SR measuring arrangement, the similar settings are selected. When measured with bias light of 505 nm, the bias voltage is 0.875 V and when measured with 770 nm bias light, a bias voltage of 0.565 V is chosen. The bias lights of 505 and 770 nm are approximated as good as possible with available filters. The filters used have their central wavelengths at 507 nm (BG 39) and at 883 nm (RG 9).

Figure 7.29 represents the SR curves of the sub cells in the organic tandem solar cell, measured with both arrangements. The maximum of the SR of the pDPP5T-2 sub cell is 0.3 A/W when measured with the accredited measuring arrangement, whereas a value of just 0.22 A/W is detected with the LED solar simulator. Also the maximum SR of the PCDTBT sub cell can be enhanced from 0.14 to 0.18 A/W when measured with the accredited measuring arrangement. However, no change in shape of curve is recognized. Only differences in the absolute height are detected. The effects of the different bias light wavelengths are assumed to be minor. The LED solar simulator thus is applicable for recording the shape of an SR curve of tandem solar cells.

These observations support the assumption, that the irradiance provided by the LED solar simulator is too low to saturate the solar cell. With a higher irradiance, a higher SR could be measured.

# 8 Discussion

**Deviation between the Spectral Response of the Tandem and Single-Junction Solar Cells**

In Figure 8.1, the SR of the tandem sub cells and the SR of the respective single-junction solar cells are opposed. Deviations are discussed below. The tandem solar cell is illuminated with monochromatic light of 20 % and bias light of 80 % intensity. The single-junction solar cells are measured only with monochromatic light of 80 % intensity.

One reason for the deviation between the SR of both cell types can be the different thickness of their active layer. The optimized layer thickness in the tandem structure (PCDTBT: 70 – 80 nm, pDPP5T-2: 80 nm) is lower than in the single-junction structure (PCDTBT: 80 nm, pDPP5T-2: 100 – 120 nm). This leads to a lower number of absorbed photons, and thus to a decrease in SR.

Another reason for the lowered SR of the tandem solar cell is the overlap of the absorption spectra of both sub cells in the wavelength rage from 400 up to approximately 700 nm. This overlap is shown as red-striped

area in Figure 8.2. The photons with low wavelength are absorbed in the PCDTBT front sub cell, and do not contribute to the current, generated by the pDPP5T-2 rear sub cell. Thus, the SR of the rear sub cell is lowered.

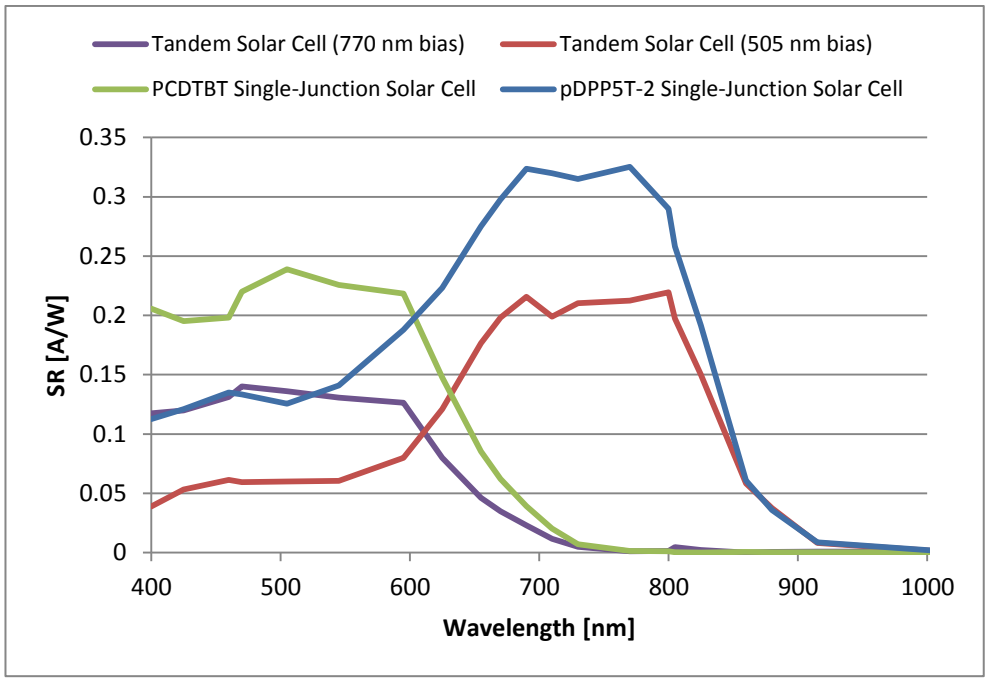


**Figure 8.1:** SR curves of the tandem solar cell with bias light at 505 nm and 770 nm compared to the SR curves of the single-junction solar cells

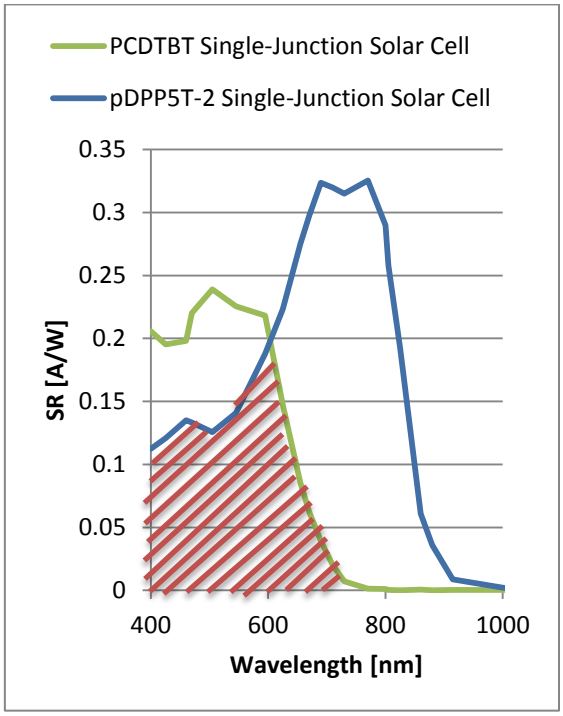


**Figure 8.2:** SR of the single-junction solar cells, indicating the lack of power for the pDPP5T-2 layer in the tandem structure

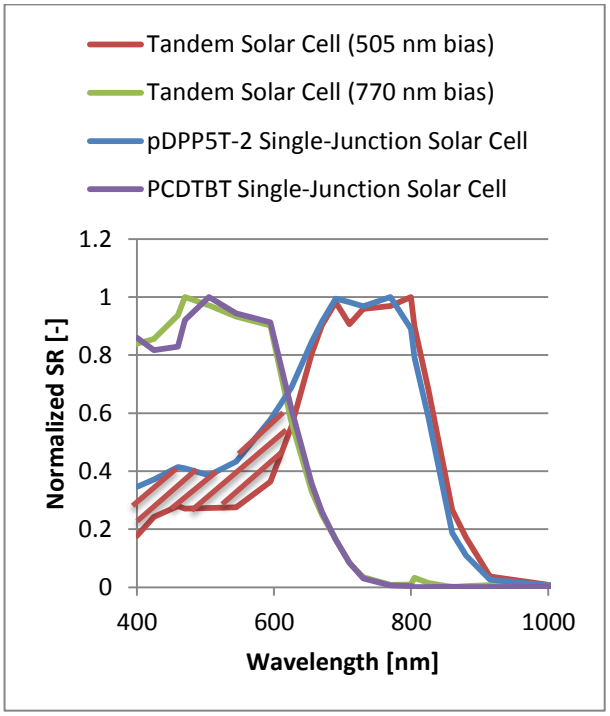


**Figure 8.3:** Normalized SR of the two sub cells in the tandem solar cell compared to the SR of the respective single-junction solar cells

Figure 8.3 shows the normalized SR of the two sub cells in the tandem solar cell and of both single-junction solar cells. The lack of SR in the rear sub cell, due to overlap of the absorption spectra, is shown as red-striped area as well. The current in the rear sub cell is reduced in the range where the front sub cell has its absorption maximum. Other differences between the normalized SR curves of both cell types are minor and can be traced back to measuring inaccuracies and morphological effects in the different cell types.

The reduction of current in the rear sub cell is also considered in the production of organic solar cells, when current-matching the sub cells of a tandem solar cell. Figure 4.7 represents the I-V-curves of all three organic solar cells under investigation. It is conspicuous, that the pDPP5T-2 single-junction solar cell is designed with a higher current than the PCDTBT single-junction solar cell. This is necessary, considering the loss of current in the pDPP5T-2 rear sub cell in a tandem structure.

Another reason for the deviation between the magnitudes of the SR of both cell types is the lack of intensity to be provided by the LED solar simulator, when measuring the SR of the tandem solar cell. In conventional SR measurement arrangements, the irradiance of the bias light is increased, until the SR curve remains constant. This condition is not fulfilled, when measuring with the LED solar simulator. Tuning of the monochromatic light intensity over 20 % for measuring the tandem solar cell is assumed to enable the detection of higher SR values.

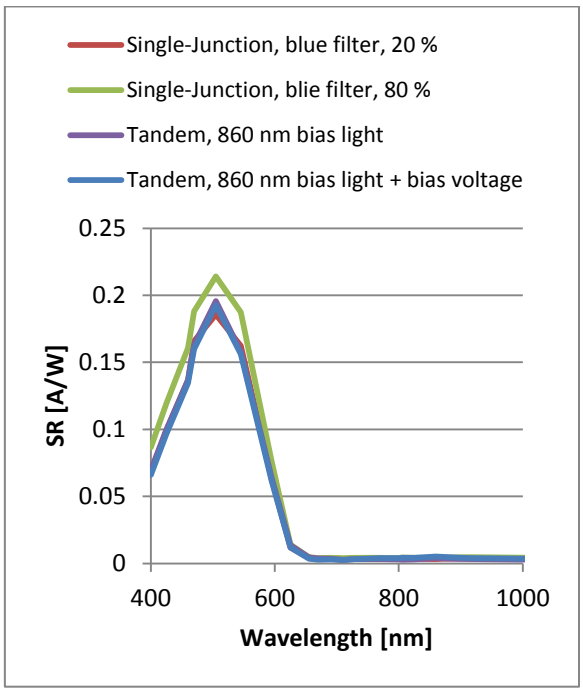


**Figure 8.4:** SR of the blue filtered single-junction silicon solar cell irradiated with monochromatic light of 20 and 80 % intensity in comparison to the SR of the blue filtered sub cell in the tandem compound

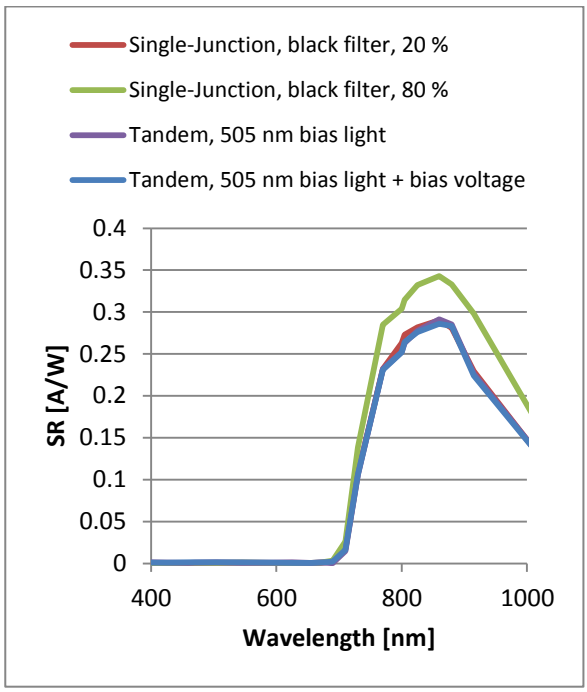


**Figure 8.5:** SR of the black filtered single-junction silicon solar cell irradiated with monochromatic light of 20 and 80 % intensity in comparison to the SR of the black filtered sub cell in the tandem compound

To prove this hypothesis, measurements are conducted with the hand-made silicon tandem solar cell. For this cell structure, the results are not influenced by effects like overlapping absorption spectra, thickness of active layer and morphological effects. Exactly the same cells are used for the tandem and for the single-junction

solar cell measurements. The absorption spectra of both sub cells do not overlap. Also, the cells are placed next to each other, and not on top of each other. Thus, the light spectrum reaching one cell is not limited by absorption in the other cell.

Figure 8.4 and Figure 8.5 represent the SR curves for the silicon single-junction solar cells, measured with monochromatic light intensity of 20, respectively 80 %, and the SR curves of the silicon tandem solar cell measured with monochromatic light intensity of 20 % and bias light intensity of 80 %. The tandem cell is measured in short circuit as well as with application of bias voltage.

Unlike when measuring the SR of an organic tandem solar cell, the bias voltage has only marginal influence on the SR of the silicon tandem solar cell. The reason is the lower slope of the I-V-curve in the range of $I_{SC.}$

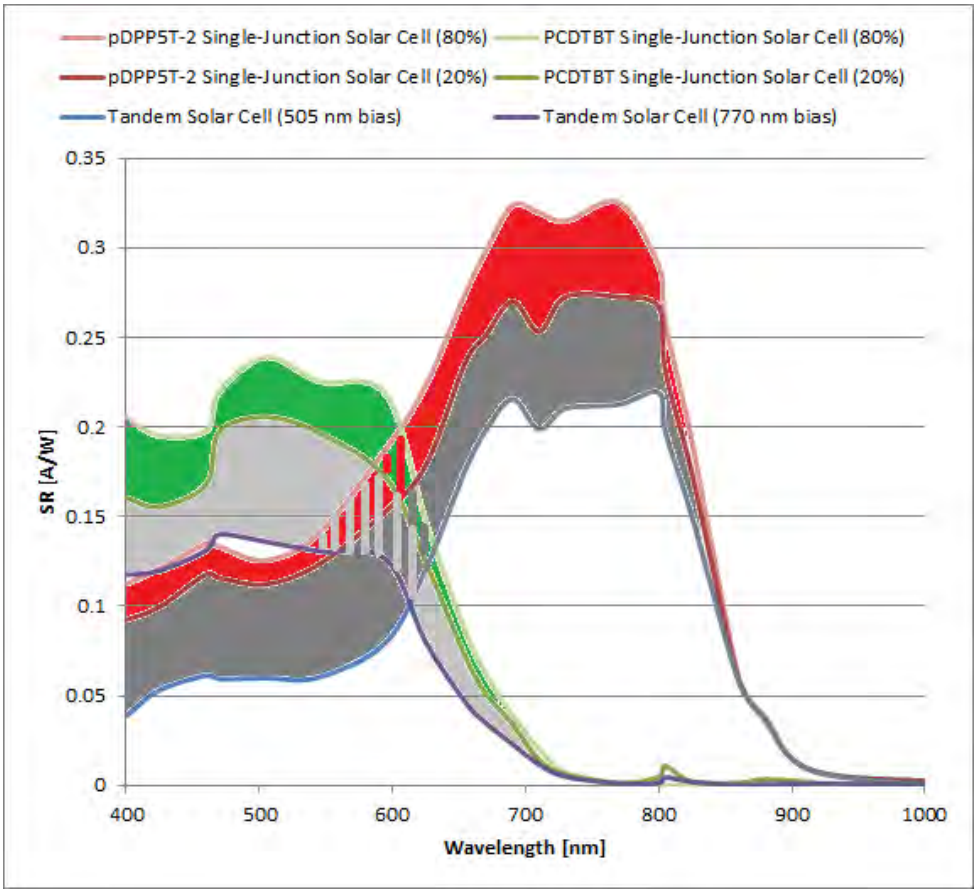


**Figure 8.6:** Differences between SR of the sub cells in the tandem solar cell and their according single-junction solar cells

The SR of the silicon tandem solar cell under given conditions highly correlates with the SR of the silicon single-junction solar cell measured with monochromatic light of 20 % intensity. The SR of the silicon tandem solar cell, however, is always lower than the SR of the silicon single-junction solar cells, when illuminated with 80 % monochromatic light intensity. In conclusion, a huge part of the difference between the SR of the organic tandem solar cell and the SR of the organic single-junction solar cells in Figure 8.1 can be traced back to the difference in light intensities. Figure 8.6 demonstrates the proportion between the error due to the

lack of light intensity (red and green), and the error due to differences in the structure (grey). When measured with only 20 % of monochromatic light intensity, the single-junction solar cell shows a lower SR, than when measured with 80 % intensity. As the SR of the tandem sub cells is even lower, the remaining losses are traced back to structural differences. The proportion of both shares is approximately equal. Thus, even when using an appropriate light intensity for the organic tandem solar cell measurement, a reduction of SR compared to the regarding organic single-junction solar cells should be recognized.

Figure 7.29 supports the assumption that the SR measured with the LED solar simulator is lower than the actual value.

**Influence of Noise on the Spectral Response**

Due to the avoidance of a chopper, the signal, especially when measuring low currents, is influenced by noise. Figure 8.7 shows a low current, depending on the voltage. The measuring object is the organic tandem solar cell from I-Meet, irradiated with monochromatic light of 595 nm (20 %) and bias light of 505 nm (80 %).

The magnitude of the noise is about $2 \cdot 10^{-7}$ A. The currents, generated by monochromatic plus bias light in an organic tandem solar cell, are in the magnitude of $2 \cdot 10^{-5}$ A - $5 \cdot 10^{-5}$ A. When corrected by the current which is generated by the bias light, the magnitude left is $2 \cdot 10^{-6}$ A - $4 \cdot 10^{-5}$ A. Latter values are used for calculation of the SR. The value of the noise is doubled, as two measuring steps, the measurement with monochromatic plus bias light and the measurement with only bias light, are necessary to obtain the SR. Hence, the noise can sum up to $4 \cdot 10^{-7}$ A. For low currents, the error can account up to 20 %. For higher SR, however, the error is decreased to 1 %. For low SR values, the error does also not gain much weight, as its effects on the SR curve can hardly be recognized. Anyway, the error caused by noise should not be underestimated.

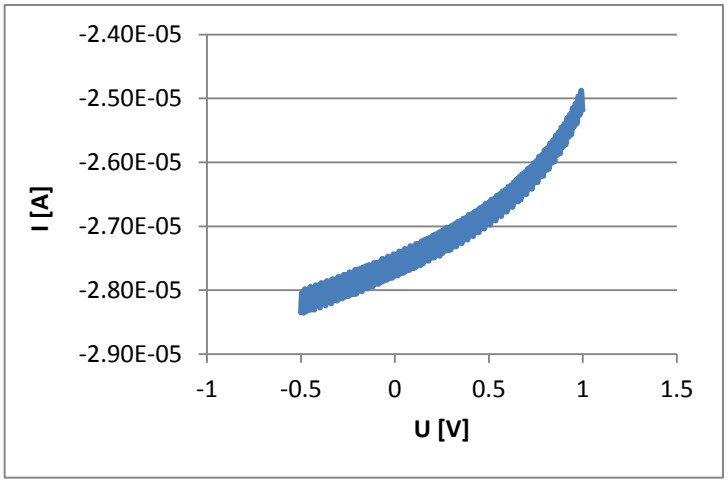


**Figure 8.7:** Noise when measuring small currents

**Errors due to Two-Point Contacting**

Due to two-point measurement, the results are influenced by the resistance of the measuring equipment. The resistance of the cables, the connecting box and the sample holder is determined by shorting the connection between two contact probes by one measuring clip, like shown in Figure 8.8.

**Figure 8.8:** Method for determination of the resistance of the measuring equipment

The resistance of the whole equipment is determined to be about 0.32 Ω. The measuring clip is considered as perfect ohmic contact with no resistance. As the series resistance of the organic solar cells is approximately between 25 (for single-junction solar cells) and 300 Ω (for tandem solar cells), the error that results from the two-point-measurement is considered negligible.

**Error due to spectral bandwidth of monochromatic light**

The spectrum emitted by the LEDs is not monochromatic, but just narrow. As the irradiance of the LED spectrum is reduced to one point of spectral maximum when evaluating the results, only an averaged value of SR over this spectral range can be determined. Thus, measurement errors can occur. For symmetric emission spectra in combination with linear SR profiles in this range, the currents generated on both sides of the central peak are equal and compensate. The same current is obtained, as under monochromatic beam conditions. Regarding to investigations of the National Renewable Energy Laboratory (NREL), by a 10 nm width of the spectrum, the same error occurs, as by a shift of the relevant wavelength by 1 nm. [47] Regarding to [48] the error due to the spectral bandwidth stays within ±2% for silicon PV, where SR is approximately linear within spectral bandwidth. No estimations for the error in organic PV can be found in literature. Thus, in following investigations, the error, caused by the spectral bandwidth of the LEDs, is considered.

The spectra, emitted by the LEDs of different wavelengths, are shown in chapter 5.1. For calibration with the reference cell, the spectral bandwidth of the LED light is taken into account. But when applying the SR of the organic solar cells in a diagram, the measured SR is reduced to one point of spectral maximum of the regarding LED. An averaged value for the SR is obtained. The error due to the spectral bandwidth of the LEDs increases for abrupt changes in SR. This is particularly the case for organic solar cells.

In Figure 8.9, the error by the spectral bandwidth for the reference cell is demonstrated. The irradiance of the LEDs, when considered as monochromatic, compared to their irradiance under consideration of the spectral shape is calculated for several intensities between 20 and 80 % and for the 21 available wavelengths between 400 and 1020 nm. Due to the insensitivity of the spectrometer in this range, no spectral shape can be recorded for 1050 nm.

Equation 21 is composed of equation 8, 9 and 10.

$$\Delta E(\lambda) = \frac{I_{SC,Ref} \cdot \int_{\lambda_{min}}^{\lambda_{max}} E_{RI}(\lambda)\, d\lambda}{\int_{\lambda_{min}}^{\lambda_{max}} E_{RI}(\lambda) \cdot SR_{Ref}(\lambda) d\lambda} - \frac{I_{SC,Ref}(\lambda)}{SR_{Ref}(\lambda)} \tag{21}$$

The deviation between both values is shown in Figure 8.9. The error bars additionally indicate the top and bottom limit of the deviation for different light intensities. The blue line represents the mean deviation for each wavelength. Especially at wavelengths, where the LED irradiance correlates not exactly linear with the intensity, the error bars are large. The large error bar at 1020 nm can be reduced to the low sensitivity of the spectrometer in this wavelength range. Thus, for 1020 and 1050 nm the irradiances without consideration of the spectral bandwidth seem more reliable.

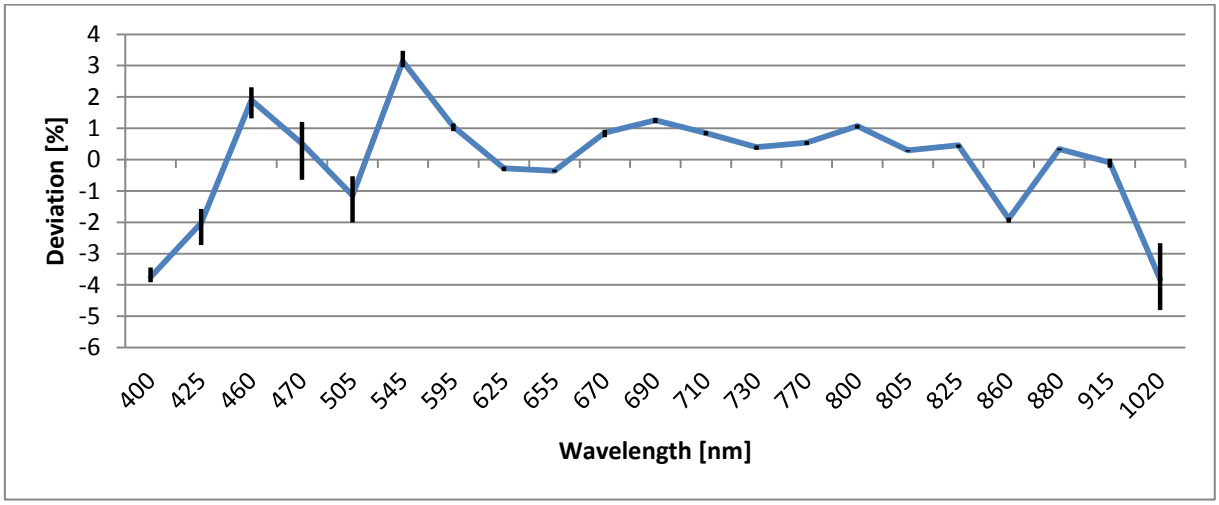


**Figure 8.9:** Deviation between the irradiance of the LEDs calculated with and without consideration of the spectral bandwidth

For positive deviation, the irradiance under consideration of the spectral bandwidth exceeds the irradiance when considering the LED radiation as monochromatic. The maximum deviation between the light irradiance

considered as monochromatic, and considered with its spectrum, amounts 4 – 5 %. For organic solar cells, however, a larger error is assumed, as its SR changes more abrupt than the SR of the silicon reference cell.

**Errors due to Inhomogeneity of Illumination**

DIN EN 60904-8 states, that the homogeneity of the illumination of the sample is especially important when the area of the cell to be measured differ from the area of the reference cell. For the LED solar simulator, not only the homogeneity of the irradiation is considered, but also the homogeneity of the distribution in colour. The LED array, used in the solar simulator, is shown in Figure 4.1. The different LEDs are not equally distributed on the array according to their wavelength. The light channel for homogenisation is only 30 cm. Thus, the incident light is still influenced by the arrangement of the LEDs on the array.

This inhomogeneity in colour was already investigated in previous studies at the ZAE. Tests were conducted for distances between the LED array and the sample, amounting 15, 25, and 50 cm. For 50 cm distance, the maximum inhomogeneity is 6.31 % at a wavelength of 805 nm. The inhomogeneity of the whole spectrum is 1.25 %. For a distance of 25 cm the maximum inhomogeneity is enhanced to 27.6 % at a wavelength of 625 nm. The inhomogeneity of the whole spectrum is increased to 2.39 %. In a light channel of 30 cm length, a maximum inhomogeneity of about 20 % is assumed. The different sizes of reference cell and test cells, as well as incorrect positioning of the sample, can lead to errors. A longer light channel is proven to increase the homogeneity.

**Errors due to Instability of Organic Solar Cells**

The stabilization of the solar cells (according to DIN EN 60904-8) is not considered. There are no reserve cells available, and damage of the samples ought to be avoided. Anyway, organic solar cells are known to be instable. This complicates reliable characterization.

Although the irradiation was kept constant for comparative measurements, the results can differ significantly. Figure 8.10 and Figure 8.11 represent measurements of both organic single-junction solar cells on different days. There are 1656 hours between Measurement 1 and Measurement 2.

All three organic solar cells degraded during the study. While the tandem solar cell and the pDPP5T-2 single-junction solar cell show only changes in their I-V-characteristics, in the PCDTBT single-junction solar cell also the shape of the SR curve is influenced by degradation. The changes in the SR characteristics are traced back to morphological modifications in the active layer. Due to entry of humidity over the ZnO layer, the crystallisation can change. The active layer consists of PCDTBT:PCBM. PCDTBT has its absorption peak at 500 nm and PCBM has its absorption peak at 250 nm. In Figure 8.11, in the second measurement an increased absorption in the low wavelength range can be detected. That can indicate an increased absorption in the PCBM after degradation. However, in Figure 8.10 only the magnitude of the SR differs. Measurement 1 is taken in a measurement series with a lot of preceding measurements. This leads to light soaking of the solar cells, as well as to heating of the sample holder. Both effects can influence the SR. With

rising temperature, the current, and hence the SR increases. However, the light soaking affects the characteristics more strongly. Thus, in both cases, the SR in Measurement 1 is decreased.

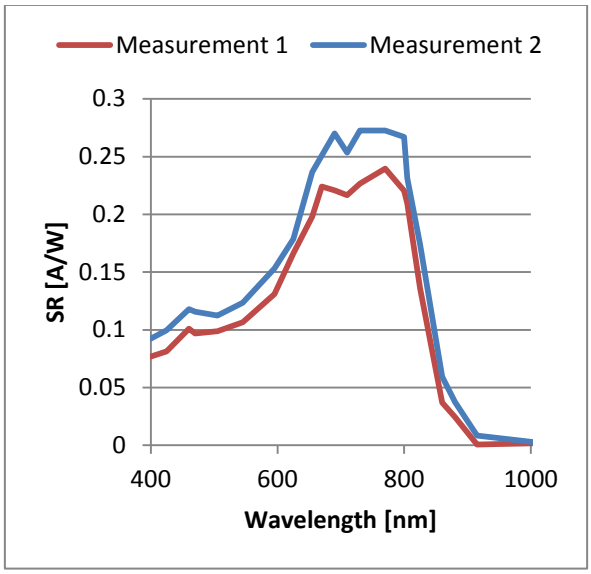


**Figure 8.10:** pDPP5T-2 single-junction solar cell under 20% monochromatic irradiation at two measuring dates lying 1656 hours apart and different pre-treatments

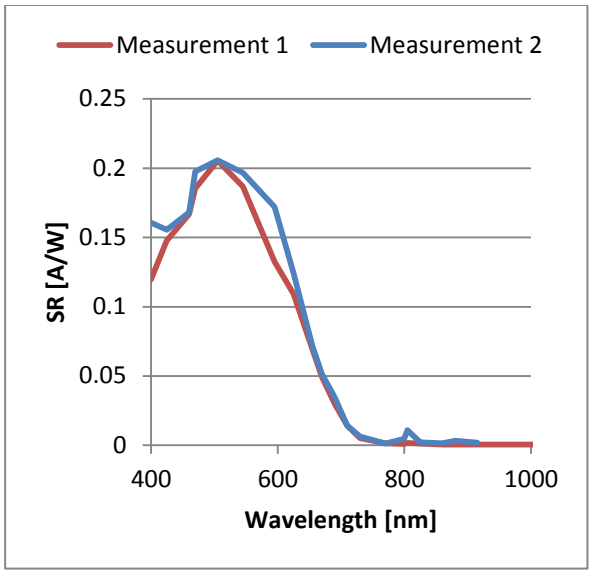


**Figure 8.11:** PCDTBT single-junction solar cell under 20% monochromatic irradiation at two measuring dates lying 1656 hours apart and different pre-treatments

Thus, the results can be influenced in two ways by the stability of the test cells. Firstly, as the different cell types are affected differently by degradation, it is difficult to compare their SR. The tandem solar cell additionally is treated with UV light. UV light soaking of the PCDTBT single-junction solar cell does not reverse the SR characteristic. Just slight improvements in the I-V-curve can be detected, when radiating single-junction solar cells with UV light.

On the other hand, the results are influenced by preceding measurements. Compared to other PV-technologies, the electrical properties of organic solar cells strongly depend on factors like e.g. storage and pre-lightning [49]. So, there can be slight variations between measurements of the same cell on different days.

**Errors due to Deviations in the Irradiance of Monochromatic Light**

Adjusting the same intensity for each LED group, does not mean, having the same irradiance at each wavelength. This can lead to errors, as higher irradiances achieve higher SRs. Figure 8.12 represents the irradiance of the LED groups at 80 % of their maximum intensity in correlation with three SR curves of tandem solar cells affected by the deviations of monochromatic light irradiance.

No correlation between the irradiance and the SR is recognized. In [46], dips of the EQE curve at wavelengths with higher monochromatic light irradiances are observed. These effects occur when the bias light intensity is too low [46].

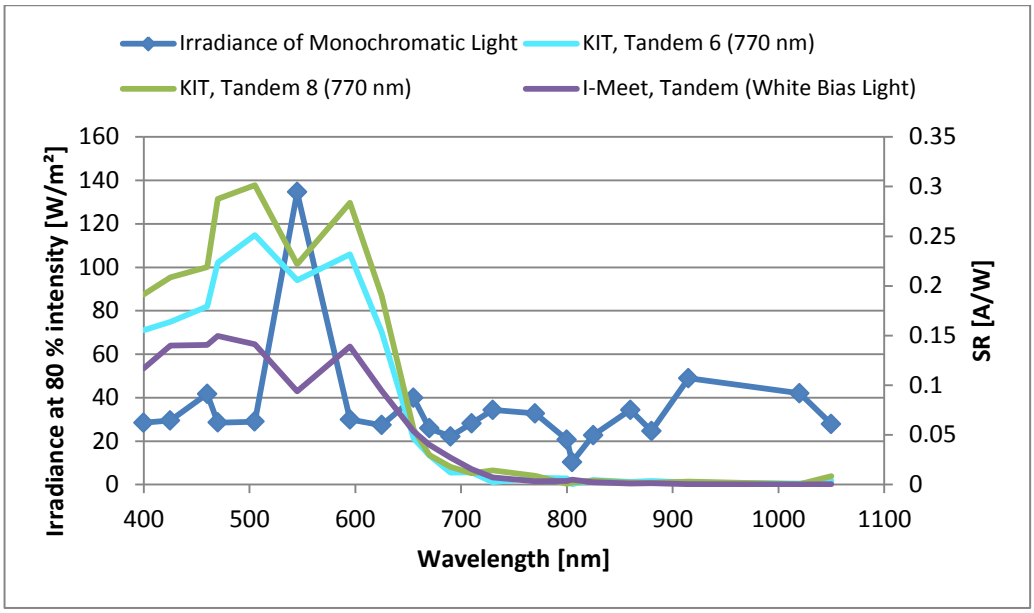


**Figure 8.12:** SR of the sub cells in the tandem structure correlated to the irradiance of monochromatic light at the different wavelengths

Errors occur only at a wavelength of 545 nm. When measuring the tandem solar cells from KIT with a bias light of 770 nm, a kink in the EQE curve is observed at 545 nm. Also, the SR curve of the tandem solar cell from I-Meet, when biased with white light, exhibits a kink at 545 nm. Thus, when the irradiance of one LED group strongly exceeds the irradiance of the LED groups at all other wavelengths, a decrease of the SR is recognized. However, at all other wavelengths the differences in irradiance are marginal and do not influence the SR. Also, in measurements where there is no absorption maximum in the range of 545 nm, no measurement artefacts are recognized at this wavelength.

**Other Impacts on Measurement Errors**

There are six cells on each sample. Thus, six different results are obtained. In the present study, the characteristics of the most stable cell are taken. Anyway, it is hard to distinguish the right cell for comparison purposes. The deviations between the $I_{SC}$ of the cells on one substrate amount up to 72 % for the pDPP5T-2, 34 % for PCDTBT, and 21.5 % for the tandem solar cell. Even on one substrate, there are huge differences. Thus, it is comprehensible that there are deviations between cells on two different substrates, respectively in two different structures (single-junction structure, tandem structure).

Another source of error is the lifting stage, which has to be readjusted for every measurement. Slight deviations cannot be avoided.

The SR curve can be inaccurate in some points, as only 22 wavelengths of monochromatic light are available. Thus, a resolution of only 22 measuring points along the x-axis is possible.

# 9 Conclusion

A novel measuring method for a solar simulator was shown with the present equipment. Influences of the intensity of monochromatic and bias light on the SR curve of an organic tandem solar cell were shown. In this respect it was found that higher SR values could be obtained with increasing monochromatic light intensity. However, the bias light must be adjusted accordingly to keep the sub cell under investigation current-limiting. Due to measurements under various conditions, the most appropriate light intensities were investigated. The wavelength for the bias light was examined by the SR of the single-junction solar cells, equivalent to the sub cells in the tandem solar cell. Unlike in conventional SR measuring arrangements, no white bias light was necessary for measuring the SR of single-junction solar cells. Thus, the SR of single-junction solar cells could be measured with just monochromatic light of high intensity. The open circuit voltage of the single-junction solar cells was used as bias voltage in SR measurements of the tandem solar cell. Comparisons between the SR of the tandem solar cell and the respective single-junction solar cells were drawn. Deviations were traced back to the differences in irradiance for both measurements as well as distinctions in structure. Assumptions were made about the sub cells of a tandem solar cell not being saturated by the irradiance applied in the SR measurement with the LED solar simulator.

Also, characteristics of organic solar cells were taken into account for interpretation of the measurement results. Effects of degradation, occurring in organic solar cells, were considered, as well as the importance of bias voltage, when measuring the SR of organic tandem solar cells.

Possible influences on measuring artefacts were taken into account. A hand-made silicon tandem solar cell was used to demonstrate the impact of the series and shunt resistance on the SR. Those parameters were shown to not influence the SR of the tandem solar cell under investigation.

Two measuring arrangements were used to provide data for comparison purposes. The results showed accordance with the SR curves recoded by the LED solar simulator, but also deviations in absolute magnitude. Uncertainties occurred when the irradiance of the monochromatic light deviated between different wavelengths.

The LED solar simulator was found a simple measuring arrangement with less components than conventional SR measuring arrangements. With the LED solar simulator, under demonstrated restrictions, the measurement of I-V-curves and SR-curves, especially for tandem solar cells, can be combined in one measuring arrangement.

Suggestions of improvements are the provision of a higher irradiance by the LED array as well as a better accordance of the irradiance at different wavelengths when tuned to the same intensity. In order to make a stronger statement about the reliability of the magnitude of the measured SR, more different cells would need to be investigated with the LED solar simulator as well as with an accredited SR measuring arrangement. Automation of the SR measurement and evaluation of the data could ease further investigations.

# Acknowledgement

With these words I want to thank my two supervisors Prof. Fritz Dildey and Ulrich Hoyer for supervising me during my master-thesis. I also want to thank the people from I-Meet who supported my work. Special thanks to Gebhart Matt and George Spyropoulos for providing information about EQE-measurements and Ning Li from I-Meet for providing the organic solar cell samples and very useful information regarding their structure and properties. Last but not least, I want to thank Konstantin Glaser from KIT for sending additional organic solar cells and useful information for comparison purposes.

# References

1. Norwood R.A., Gangopadhay P. and Shahin S., 2012, Ultra-thin organic photovoltaics with increased efficiency, SPIE Newsroom. DOI: 10.1117/2.1201212.004593
2. Benanti T.L., Venkataraman D., 2006, Organic solar cells: An overview focusing on active layer morphology, Photosynth. Res., 87, p. 73-81
3. Choy Wallace C.H., Organic Solar Cells: Materials and Device Physics, Springer London Ltd, 2012
4. Prall H.-J., Koeppe R., Autengruber R., Egginger M., Dennler G., Sariciftci N.S., 2006, From evaporation to solution processed organic tandem solar cells, 61970F, Gombert, Andreas, Strasbourg, France
5. Zhang C., Hao Y., Chen D., Wang Z. and Lin Z., Investigation of Organic Bulk Heterojunction Solar cells from optical aspect, Solar Cells – Research and Application Perspectives, Prof. Arturo Morales-Acevedo (Ed.), InTech, DOI: 10.5772/52819
6. Zimmermann B., Würfel U. and Niggemann M., 2009, Long term stability of efficient inverted P3HT:PCBM solar cells, Sol. Energy Mater. Sol. Cells, 93, p. 491–496
7. Kim C.S., Lee S.S., Gomez E.D., Kim J.B., and Loo Y.L., 2009, Transient photovoltaic behaviour of air-stable, inverted organic solar cells with solution-processed electron transport layer, Appl. Phys. Lett., 94, 113302
8. Ameri T., Dennler G., Waldauf C., Azimi H., Seemann A., Forberich K., Hauch J., Scharber M., Hingerl K. and Brabec C.J., 2010, Fabrication, optical modeling and color characterization of semitransparent bulk-heterojunction organic solar cells in an inverted structure, Adv. Funct. Mater., 20, p. 1592 - 1598
9. Kim J.Y., Lee K., Coates N.E., Moses D., Nguyen T.Q., Dante M. and Heeger A.J., 2007, Efficient tandem polymer solar cells fabricated by all-solution processing, Science, 317, p. 222–225
10. Sista S., Hong Z., Park M.-H., Xu Z. and Yang Y., 2010, High-efficiency polymer tandem solar cells with three-terminal structure, Adv. Mater., 22, p. E77 – E80
11. Chen L.M., Hong Z.R., Li G. and Yang Y., 2009, Recent progress in polymer solar cells: manipulation of polymer: fullerene morphology and the formation of efficient inverted polymer solar cells, Adv. Mater., 21, p. 1434 – 1449

12. Hau S.K., Yip H.-L., Ma H. and Jen A.K.-Y., 2008, High performance ambient processed inverted polymer solar cells through interfacial modification with a fullerene self-assembled monolayer, Appl. Phys. Lett., 93, 233304
13. Hsieh C.-H., Cheng Y.-J., Li P.-J., Chen C.-H., Dubosc M., Liang R.-M. and Hsu C.-S., 2010, Highly efficient and stable inverted polymer solar cells integrated with a cross-linked fullerene material as an interlayer, J. Am. Chem. Soc., 132, p. 4887 – 4893
14. Liao H.-H., Chen L.-M., Xu Z., Li G. and Yang Y., 2008, Highly efficient inverted polymer solar cell by low temperature annealing of Cs2CO3 interlayer, Appl. Phys. Lett., 92, 173303
15. Dennler G., Scharber M. and Brabec C., 2009, Polymer-fullerene bulk-heterojunction solar cells, Adv. Mater., 21, p. 1323 - 1338
16. Gadisa A., Liu Y., Samulski E.T., Lopez R., 2012, Role of thin n-type metal-oxide interlayers in inverted organic solar cells, Appl. Mater. Interfaces, 4, p. 3846 – 3851
17. Green M.A., Emery K., Hishikawa Y., Warta W., Dunlop E.D.,2013, Solar Cell Efficiency Tagles (Version 41), Prog. Photovoltaics, 21, p. 1 - 11
18. Seifer H., Hohl-Ebinger J., Uhrich C., Timmreck R., Riede M., Warta W., 2010, Spectrometric characterization of multi-junction organic solar cells, 25th European PV Solar Energy Conference and Exhibition, 6-10 September 2010, Valencia, Spain, p. 813 - 818
19. Li N., Baran D., Forberich K., Machui F., Ameri T., Turbiez M., Carrasco-Orozco M., Drees M., Facchetti A-, Krebs F.C. and Brabec C.J., 2013, Towards 15% energy conversion efficiency: a systematic study of the solution-processed organic tandem solar cells based on commercially available materials, Energy Environ. Sci., 6, p. 3407 - 3413
20. Kouijzer S., Esiner S., Frijters C.H., Turbiez M., Wienk M.M., Janssen R.A.J., 2012, Efficient Inverted Tandem Polymer Solar Cells with a Solution-Processed Recombination Layer, Advanced Energy Materials, 2, p. 945 – 949
21. Repmann T., Kirchhoff J., Reetz W., Birmans F., Müller J., Rech B., 2003, Investigations on the current matching of highly efficient tandem solar cells based on amorphous and microcrystalline silicon, Proceedings of 3rd World Conference on Photovoltaic Energy Conversion, Osaka, Japan, 2, p. 1843 - 1846
22. Dou L., You J., Yang J., Chen C.-C., He Y., Murase S., Moriarty T., Emery K., Li G., and Yang Y., 2012, Tandem polymer solar cells featuring a spectrally matched low-bandgap polymer, Nat. Photon., 6, p. 180 - 185
23. Dennler G., Scharber M.C., Ameri T., Denk P., Forberich K., Waldauf C., Brabec C.J., 2008, Design Rules for Donors in Bulk-Heterojunction Tandem Solar Cells Towards 15 % Energy-Conversion Efficiency, Adv. Mater., 20, p. 579 - 583
24. Minnaert B., Veelaert P., 2012, Guidelines for the Bandgap Combinations and Absorption Windows for Organic Tandem and Triple-Junction Solar Cells, Materials , 5, p. 1933 - 1953
25. Wagemann H.-G. ; Eschrich H., Photovoltaik, GWV Fachverlage GmbH, Wiesbaden 2010, p. 53
26. Mertens K., Photovoltaik - Lehrbuch zu Grundlagen, Technologie und Praxis, Carl Hanser Verlag, 2013, p. 90

27. Park S. H., Roy A., Beaupre S., Cho S., Coates N., Moon J. S., Moses D., Leclerc M., Lee K. and Heeger A. J., 2009, Bulk Heterojunction Solar Cells With Internal Quantum Efficiency Approaching 100%, Nat. Photon., 3, p. 297-303
28. Deibel C., 2008, Intermediate: Current-Voltage Characteristics of Organic Solar Cells, http://blog.disorderedmatter.eu/2008/03/05/intermediate-current-voltage-characeristics-of-organic-solar-cells/ , 26.02.14
29. Dibb G.F.A. et al., 2013, Influence of doping on charge carrier collection in normal and inverted geometry polymer:fullerene solar cells. Sci. Rep. 3, 3335
30. Schädel M., Isenberg J., Suthues J., Ballif C., Gobsch G., Improving quantum efficiency measurement in large area solar cells by using appropriate bias illumination, Proceedings of the 21th European Photovoltaic Solar Energy Conference, September 4-8, 2006 Dresden, p. 1 - 4
31. Luque A., Hegedus S., Handbook of Photovoltaic Science and Engineering, Wiley, 2011
32. Pravettoni M., Galleano R., Virtuani A., Müllejans H., Dunlop E.D., 2011, Spectral response measurement of double-junction thin-film photovoltaic devices: the impact of shunt resistance and bias voltage, Meas. Sci. Technol., 22, 045902
33. Gilot J., Wienk M.M., Janssen R.A.J., 2010, Measuring the external quantum efficiency of two-terminal polymer tandem solar cells, Adv. Energy Mat., 20, p. 3904 - 3911
34. Collins S., Chapman E., Dye Sensitized Solar Cells, 2008, http://www.cornellcollege.edu/physics/courses/phy312/Student-Projects/Solar-Cell/Solar-Cell.html, 17.03.2014
35. Swonke T., Hoyer U., Concept for a Real AM1.5 Simulator Based on LED-Technology And Survey on Different Types of Solar Simulators, 24th European Photovoltaic Solar Energy Conference, 21.-25.09.2009, Hamburg, Deutschland, p. 3377 - 3379
36. Silvestre S., Sentis L. Castaner L., 1999, A fast low-cost solar cell spectral response measurement system with accuracy indicator, IEEE T. Instrumentation and Measurement, 48, p. 944 - 948
37. EN 60904-8 “Photovoltaic device – Part 8: Measurement of spectral response of a photovoltaic (PV) device
38. Herguth A., Raabe B., Scholz S., Hahn G., Haverkamp H., Nissler R., Habermann D., Buchner C., Schmid C., 2011, Influence of spectral mismatch, cell reflection properties and IQE on the efficiency measurement, 26th European Photovoltaic Solar Energy Conference and Exhibition, Hamburg, p. 1555 - 1557
39. Newport Corporation, Application Note 51, The Spectral Mismatch Factor, http://www.newport.com/images/webDocuments-EN/images/Spectral_Mismatch-App_Note_51.pdf, 17.03.2014
40. Gilot J., Wienk M.M. and Janssen R.A.J., 2007, Double and triple junction polymer solar cells processed from solution, Appl. Phys. Lett., 90, 143512
41. Beek W.J.E., M. Wienk M.M., Kemerink M., Yang X.N., and Janssen R.A.J., 2005, Hybrid zinc oxide conjugated polymer bulk heterojunction solar cells, J. Phys. Chem. B., 109, p. 9505 - 9516
42. Verbakel F., Meskers S.C.J., and Janssen R.A.J., 2006, Electronic memory effects in diodes from a zinc oxide nanoparticle-polystyrene hybrid material, Appl. Phys. Lett., 89, 102103

43. Yuan Y., Huang J., Li G., 2011, Intermediate Layers in Tandem Organic Solar Cells, Green, 1, pp. 65-80
44. Böttcher A., Prorok A., Ferretti N., Preiss A., Krauter S., Grunow P., Flasher tolerances of power measurement on micromorph tandem modules, 25th European Solar Energy Conference and Exhibition, 6-10 September 2010, Valencia, Spain, p. 3161-3164
45. Meusel M., Adelhelm R., Dimroth F., Bett A.W. and Warta W., 2002, Spectral Mismatch Correction and Spectrometric Characterization of Monolithic III-V Multi-Junction Solar Cells, Progress in Photovoltaics: Research and Applications, 10, p. 243 - 255
46. Meusel M., Baur C., Létay G., Bett A.W. and Warta W., 2003, Spectral Response Measurements of Monolithic GaInP/Ga(In)As/Ge Triple-Junction Solar Cells – Measurement Artifacts and their Explanation, Progress in Photovoltaics: Research and Applications, 11, p. 499 - 514
47. Field H., Solar Cell Spectral Response Measurement Errors Related to Spectral Band Width and Chopped Light Waveform, Conference Record of the 26$^{th}$ IEEE Photocoltaic Specialists Conference, 29.09.-03.10.1997, Anaheim, CA , USA, p. 471-474
48. Zaid G., Park S.-N., Park S., and Lee D.-H., 2010, Differential spectral responsivity measurement of photovoltaic detectors with a light-emitting-diodebased integrating sphere source, Appl. Optics, 49, p. 6772 - 6783
49. Markvart T., Castaner L., Practical Handbook of Photovoltaics: Fundamentals and Applications, Elsevier, Oxford, 2003, p. 483-497

# List of Figures

# Statement of Affirmation

I hereby declare that the master thesis submitted was in all parts exclusively prepared on my own, and that other resources or other means (including electronic media and online sources), than those explicitly referred to, have not been utilized.

All implemented fragments of text, employed in a literal and/or analogous manner, have been marked as such.

Erlangen, 25.03.2014 Christiane Dettelbacher

# Appendix

## A Full Width at Half Maximum of Light Emitted by all 22 LEDs

**Table 2:** FWHM of the Light emitted by the different LED groups used in the LED solar simulator at 100 % intensity

| Wavelength [nm] | FWHM [nm] |
|---|---|
| **400** | 14.5 |
| **425** | 18.5 |
| **460** | 20.5 |
| **470** | 24 |
| **505** | 38.25 |
| **545** | 71 |
| **595** | 16.5 |
| **625** | 21 |
| **655** | 23 |
| **670** | 21.5 |
| **690** | 23 |
| **710** | 25 |
| **730** | 25.5 |
| **770** | 26.5 |
| **800** | 29.5 |
| **805** | 27 |
| **825** | 29.75 |
| **860** | 33.75 |
| **880** | 31.5 |
| **915** | 48 |
| **1020** | 22.75 |
| **1050** | - |

# B Calibration Certificate of the Reference Cell

DEUTSCHER KALIBRIERDIENST **DKD**

Kalibrierlaboratorium / *Calibration laboratory*

Akkreditiert durch die / *accredited by the*
Akkreditierungsstelle des Deutschen Kalibrierdienstes

**ISE CalLab PV Cells**
**Heidenhofstr. 2**
**79110 Freiburg**

Fraunhofer ISE

CalLab PV Cells

Deutscher Akkreditierungs Rat DAR

DKD-K-47101

| 3001061ZAE |
|---|
| DKD-K-47101 |
| 2013-03 |

Kalibrierschein
*Calibration certificate*

Kalibrierzeichen
*Calibration mark*

| | |
|---|---|
| Gegenstand<br>*Objekt* | **Referenzsolarzelle** |
| Hersteller<br>*Manufacturer* | - |
| Typ<br>*Type* | **monokristallines Silicium** |
| Fabrikat/Serien-Nr.<br>*Serial number* | **ZAE001 / 10510-0372** |
| Auftraggeber<br>*Customer* | **Bayerisches Zentrum für Angewandte Energieforschung**<br>**Haberstr. 2 a**<br>**91058 Erlangen** |
| Auftragsnummer<br>*Order No.* | **061ZAE0313** |
| Anzahl der Seiten des Kalibrierscheins<br>*Number of pages of the certificate* | **4** |
| Datum der Kalibrierung<br>*Date of calibration* | **04.07.2013** |

Dieser Kalibrierschein dokumentiert die Rückführung auf nationale Normale zur Darstellung der Einheiten in Übereinstimmung mit dem Internationalen Einheiten-system (SI).
Der DKD ist Unterzeichner der multilateralen Übereinkommen der European co-operation for Accreditation (EA) und der International Laboratory Accreditation Cooperation (ILAC) zur gegenseitigen Anerkennung der Kalibrierscheine.
Für die Einhaltung einer angemessenen Frist zur Wiederholung der Kalibrierung ist der Benutzer verantwortlich.
*This calibration certificate documents the traceability to national standards, which realize the units of measurement according to the International System of Units (SI).*
*The DKD is signatory to the multilateral agreements of the European co-operation for Accreditation (EA) and of the International Laboratory Accreditation Cooperation (ILAC) for the mutual recognition of calibration certificates.*
*The user is obliged to have the object recalibrated at appropriate intervals.*

Dieser Kalibrierschein darf nur vollständig und unverändert weiterverbreitet werden. Auszüge oder Änderungen bedürfen der Genehmigung sowohl der Akkreditierungsstelle des DKD als auch des ausstellenden Kalibrierlaboratoriums. Kalibrierscheine ohne Unterschrift und Stempel haben keine Gültigkeit.
*This calibration certificate may not be reproduced other than in full except with the permission of both the Accreditation Body of the DKD and the issuing laboratory. Calibration certificates without signature and seal are not valid.*

| Stempel<br>*Seal* | Datum<br>*Date* | Leiter des Kalibrierlaboratoriums<br>*Head of the calibration laboratory* | Bearbeiter<br>*Person in charge* |
|---|---|---|---|
| Deutscher Kalibrierdienst DKD-K-47101 | 09.07.2013 | Wilhelm Warta | Astrid Semeraro |

Fraunhofer ISE

CalLab PV Cells

| 3001061ZAE |
|---|
| DKD-K-47101 |
| 2013-03 |

## 1. Beschreibung des Kalibriergegenstandes

*Description of the calibration object*

Das Kalibrierobjekt besteht aus einer Solarzelle Typ: monokristallines Silicium, die mit einem Glas in einem Gehäuse eingegossen ist. Die Vorderseiten- sowie die Rückseitenkontakte der Zelle sind wie die Temperaturerfassung über einen Steckkontakt zugänglich. Die Temperaturerfassung erfolgt mittels eines internen Pt 100 -Sensors. Die Stabilität der Solarzelle wurde nicht untersucht.

## 2. Messverfahren

*Measurement procedure*

Bestimmt wird der Wert der absoluten differentiellen spektralen Empfindlichkeit im Wellenlängenbereich ca. 300-1200 nm bei einem Kurzschlussstrom, so dass diese mit der absoluten spektralen Empfindlichkeit bei Standard Test Bedingungen übereinstimmt. Die Kalibrierung der Solarzelle wurde mit einem Filtermonochromator mit dem DSR-Messverfahren /1/ und entsprechend /2/ durchgeführt. Die Messung wird im Zweistrahlverfahren durchgeführt und verwendet gleichzeitig:
a) eine stationäre Biasbestrahlung mit Bestrahlungsstärken $E_B$, welche jedoch nicht explizit gemessen werden. Ihre Variation erlaubt unterschiedliche Kurzschlussströme $I_{SC}$ ($E_B$), sowie
b) eine zeitlich modulierte, quasi-monochromatische Messstrahlung. Ihre Bestrahlungsstärke wird bestimmt mit einer primarkalibrierten Referenzsolarzelle (PTB):

Rückführung der Referenzsolarzelle:

| Identitäts-Nr.: | Kalibrierschein-Nr.: | Rückführung: |
|---|---|---|
| 025-2010 | 47178-PTB-10 | PTB |

Mittels einer zeitlich modulierten sonnenähnlichen Messstrahlung wird durch zusätzliche Variation der Biasbestrahlungstärke ($E_B$) die Linearität der Solarzelle ermittelt. Für den Fall eines nichtlinearen Messobjektes wird so eine Biasbestrahlungsstärke bestimmt, bei welcher der Wert der absoluten differentiellen spektralen Empfindlichkeit, mit dem der absoluten spektralen Empfindlichkeit bei Standard Test Bedingungen übereinstimmt /3/. Alle verwendeten Prüfmittel unterliegen einer Prüfmittelüberwachung nach ISO 9001:2008. Insbesondere liegen für alle relevanten Einzelkomponenten des verwendeten Filtermonochromator-Aufbaus Kalibrierzertifikate bei externer Kalibrierung bzw. interne Kalibrierprotokolle vor.

## 3. Messbedingungen

Measurement conditions

Der Arbeitspunkt der Solarzelle wird durch den Bias-Strom im $I_{SC}$ definiert.

| | |
|---|---|
| Bias Strom: | 10 mA |
| Nominalwert der Temperatur des Messobjekts: | 25 °C |

Die Klemmenspannung der Solarzelle wird durch einen Strom-Spannungswandler auf unter 0.03 $V_{OC}$ geregelt. Die Frequenz des getakteten quasimonochromatischen Messlichtes lag bei 117 Hz. Die spektrale Bandbreite (Halbwertsbreite) der Filter liegt unter 15 nm und hat einen Öffnungswinkel zwischen den Randstrahlen von maximal 5°. Die Temperatur der Solarzelle wird mittel einem Tastsensor ermittelt und auf (25±0.5)°C eingestellt.

Seite 3
*Page*

Fraunhofer ISE

CalLab PV Cells

| 3001061ZAE |
|---|
| DKD-K-47101 |
| 2013-03 |

## 4. Messergebnis
*Measurement result*

| Wellenlänge [nm] | *$\eta_{ext}$ [%] | *s* [mA*m²/W] | **rel. Messunsicherheit [%] | Messunsicherheit [mA*W⁻¹*m²] |
|---|---|---|---|---|
| 297.0 | 42.4 | 0.5 | 11 | 0.0045 |
| 309.2 | 42.7 | 0.0426 | 9 | 0.0038 |
| 321.2 | 43.5 | 0.0451 | 9 | 0.0041 |
| 330.8 | 44.2 | 0.0472 | 9 | 0.0042 |
| 340.3 | 44.8 | 0.0492 | 9 | 0.0044 |
| 369.2 | 48.3 | 0.0575 | 9 | 0.0052 |
| 399.3 | 61.0 | 0.0786 | 9 | 0.0071 |
| 425.7 | 69.3 | 0.0951 | 2 | 0.0019 |
| 452.3 | 74.7 | 0.1090 | 2 | 0.0022 |
| 474.3 | 77.5 | 0.1186 | 2 | 0.0024 |
| 498.8 | 79.6 | 0.1280 | 2 | 0.0026 |
| 523.7 | 80.9 | 0.1368 | 2 | 0.0027 |
| 548.8 | 81.4 | 0.1442 | 2 | 0.0029 |
| 575.8 | 82.4 | 0.1531 | 2 | 0.0031 |
| 601.7 | 82.5 | 0.1602 | 2 | 0.0032 |
| 621.3 | 82.7 | 0.1657 | 2 | 0.0033 |
| 649.2 | 82.8 | 0.1734 | 2 | 0.0035 |
| 699.1 | 82.7 | 0.1864 | 3 | 0.0056 |
| 742.4 | 82.5 | 0.1977 | 3 | 0.0059 |
| 767.6 | 82.4 | 0.2041 | 3 | 0.0061 |
| 790.0 | 82.0 | 0.2090 | 3 | 0.0063 |
| 809.9 | 81.3 | 0.2125 | 3 | 0.0064 |
| 827.2 | 80.7 | 0.2154 | 3 | 0.0065 |
| 842.3 | 80.3 | 0.2181 | 3 | 0.0065 |
| 859.8 | 79.2 | 0.2197 | 3 | 0.0066 |
| 881.6 | 77.7 | 0.2210 | 3 | 0.0066 |
| 906.4 | 75.6 | 0.2212 | 3 | 0.0066 |
| 928.8 | 73.0 | 0.2188 | 3 | 0.0066 |
| 948.7 | 70.0 | 0.2142 | 3 | 0.0064 |
| 974.5 | 64.8 | 0.2039 | 3 | 0.0061 |
| 998.1 | 58.9 | 0.1896 | 3 | 0.0057 |
| 1015.9 | 53.8 | 0.176 | 10 | 0.018 |
| 1026.0 | 50.5 | 0.167 | 10 | 0.017 |
| 1050.4 | 40.8 | 0.138 | 10 | 0.014 |
| 1060.9 | 35.4 | 0.121 | 10 | 0.012 |
| 1067.0 | 32.6 | 0.112 | 10 | 0.011 |
| 1111.5 | 16.0 | 0.057 | 19 | 0.011 |
| 1121.6 | 12.7 | 0.0460 | 19 | 0.0087 |
| 1136.4 | 8.52 | 0.0312 | 19 | 0.0059 |
| 1164.1 | 2.65 | 0.0100 | 75 | 0.0075 |
| 1185.9 | 0.332 | 0.0013 | 206 | 0.0026 |

*Spektrale Empfindlichkeit und externe Quanteneffizienz stehen in folgendem Zusammenhang:

mit c Vakuumlichtgeschwindigkeit
h Planck'sches Wirkungsquantum
q Elementarladung
n Brechungsindex Luft

$$\eta_{ext}(\lambda) = \frac{J(\lambda)/q}{E(\lambda)/h\nu} = \frac{h\nu}{q}\frac{J(\lambda)}{E(\lambda)} = \frac{hc}{nq\lambda}\frac{s(\lambda)}{a} = 1239{,}8\frac{nm\cdot W}{A}\frac{s(\lambda)}{n\lambda a}$$

$\eta_{ext}(\lambda)$: externe Quanteneffizienz s(λ): spektrale Empfindlichkeit a: Fläche

**Angegeben ist jeweils die erweiterte Messunsicherheit , die sich aus der Standardmessunsicherheit durch Multiplikation mit dem Faktor k=2 ergibt. Sie wurde gemäß dem "Guide to the expression of Uncertainty in Measurement" ermittelt.
Sie entspricht bei einer Normalverteilung der Abweichungen vom Messwert einer Überdeckungswahrscheinlichkeit von 95%.

Fraunhofer ISE

CalLab PV Cells

| 3001061ZAE |
| --- |
| DKD-K-47101 |
| 2013-03 |

**5. Zusatzinformationen:**

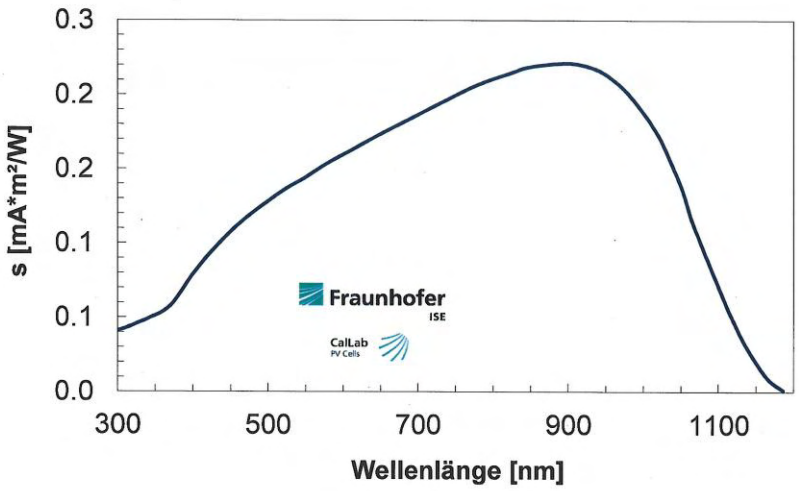


**6. Literatur:**

/1/ J. Metzdorf, Calibration of Solar Cells. 1: *The Differential Spectral Responsivity Method*, Applied Optics 26 (1987) p.1701-1708

/2/ IEC 60904-8:1998, Photovoltaic devices - Part 8: *Measurement of the spectral response of a photovoltaic (PV) device*

/3/ J. Hohl-Ebinger, G. Siefer, and W. Warta., *Non-Linearity of Solar Cells in Spectral Response Measurements.* in 22th European Photovoltaic Solar Energy Conference and Exhibition. 2007.